ORBITAL LIFETIME ANALYSES OF PICO- AND NANO-SATELLITES

By

AI-AI LUMNAY C. COJUANGCO

A THESIS PRESENTED TO THE GRADUATE SCHOOL
OF THE UNIVERSITY OF FLORIDA IN PARTIAL FULFILLMENT
OF THE REQUIREMENTS FOR THE DEGREE OF
MASTER OF SCIENCE

UNIVERSITY OF FLORIDA

2007

To my mother and sister

ACKNOWLEDGMENTS

I extend my sincere gratitude to my advisor, Dr. Norman Fitz-Coy, for his generous support, guidance and patience through my graduate studies at the University of Florida.

I acknowledge and give appreciation to my committee members Dr. John K. Schueller and Dr. Carl Crane for providing valuable input to this work.

I acknowledge my colleagues in the AMAS lab, the Space Systems Group and SAMM group, for their support, input, and company with research and graduate studies.

I express my appreciation to the women in my life group, Pascalie Belony, Jamie Cabug, Ann Duong, Sunny Ho, Jenny Jose, Christine Moran, and Carrie Torbert for their continuous encouragement, belief in me, words of wisdom, prayers, and for being such great inspirations to my life since I arrived at University of Florida. Also, to all the wonderful people I have met and befriended through Gator Christian Life.

I thank Cris Dancel for her time, guidance and support with this work. I also express my appreciation to the rest of the Filipino community I have met here for making me feel at home. I thank my friends in Illinois as well for keeping me in their thoughts.

I thank my family. I especially thank my mother, Evangeline Chongco, and sister, Claudine Foronda, for their love, support, and for allowing me to pursue graduate studies.

Last, I express my deep gratitude to Jesus Christ, my Lord, my Savior and my God, it is through Him I have faith and strength and it is He who has made all of this possible. I thank Him for his beautiful creation that I have had the joy in living and learning about.

TABLE OF CONTENTS

page

ACKNOWLEDGMENTS 4

LIST OF TABLES 7

LIST OF FIGURES 8

ABSTRACT 9

CHAPTER

1 INTRODUCTION AND BACKGROUND 11

Definition of Orbital Debris 11
Concerns with Orbital Debris 11
Development of Mitigation Guidelines 15
Motivation of Research 17

2 METHODS 20

Two-body Problem 20
Conic Sections 23
Orbital Elements 25
Perturbations 26
Perturbation Techniques 30
Orbital Lifetime 33

3 SIMULATIONS USING SATELLITE TOOL KIT (STK) SOFTWARE 35

Satellite Tool Kit (STK) 35
STK Lifetime Tool 35
STK Satellite Properties 39
Parameter Sensitivity Study 41

4 RESULTS AND DISCUSSION 46

Pico-satellite Results 46
Nano-satellites Results 50

5 CONCLUSION AND RECOMMENDATIONS 58

Conclusions 58
Recommendations 59

LIST OF REFERENCES 60

BIOGRAPHICAL SKETCH 63

LIST OF TABLES

Table		page
3-1	Satellite mass, drag area, and area exposed to Sun	37
3-2	Orbital lifetime sensitivity simulation parameters	41
4-1	CubeSat simulation parameters	47
4-2	MR SAT and MRS SAT simulation parameters	51
4-3	FASTRAC simulation parameters	51
4-4	Akoya-B and Bandit-C simulation parameters	52
4-5	MR SAT with different initial altitudes simulation parameters	52

LIST OF FIGURES

Figure		page
1-1	Typical pico- and nano-class satellite mass, volume and power ratios	18
1-2	Computer generated image of orbital debris in LEO	19
2-1	Relative motion of two-bodies	21
2-2	Geometry of an elliptic conic section	24
2-3	Orbital elements	25
3-1	STK Lifetime tool GUI	36
3-2	STK Lifetime Advanced option GUI	39
3-3	STK satellite properties GUI	40
3-4	Orbital lifetime vs. reflection coefficient	43
3-5	Orbital lifetime vs. area exposed to Sun	43
3-6	Orbital lifetime vs. drag coefficient	44
3-7	Orbital lifetime vs. drag area	44
3-8	Orbital lifetime vs. mass	45
4-1	Orbital lifetime results for satellite A using seven atmospheric density models	48
4-2	Orbital lifetime results for satellite C using seven atmospheric density models	48
4-3	Orbital lifetime results for satellites A, B, C, and D at 600-km initial altitude	49
4-4	Orbital lifetime for MR SAT and MRS SAT at 350-km initial altitude	54
4-5	Orbital lifetime for MR SAT and MRS SAT at 750-km initial altitude	55
4-6	Orbital lifetime for the FASTRAC satellites at 350-km initial altitude	55
4-7	Orbital lifetime for the FASTRAC satellites at 750-km initial altitude	56
4-8	Orbital lifetime for the Akoya-B and Bandit-C at 350-km initial altitude	56
4-9	Orbital lifetime for the Akoya-B and Bandit-C at 750-km initial altitude	57
4-10	Orbital lifetime for the MR SAT using different initial altitudes	57

Abstract of Thesis Presented to the Graduate School
of the University of Florida in Partial Fulfillment of the
Requirements for the Degree of Master of Science

ORBITAL LIFETIME ANALYSES OF PICO- AND NANO-SATELLITES

By

Ai-Ai Lumnay C. Cojuangco

December 2007

Chair: Norman Fitz-Coy
Major: Mechanical Engineering

In recent years, orbital debris has been a growing concern for the space industry due to its potential risk of causing collisions. Several agencies and organizations, such as the National Aeronautics and Space Administration (NASA), and the United Nations Committee on the Peaceful Uses of Outer Space (UNCOPUOS), have been involved in studying orbital debris and developing mitigation guidelines. In 2004, the Federal Communications Commission (FCC) began requiring a debris mitigation plan for all non-government United States radio communication satellites to be launched into orbit.

Orbital lifetime analysis of a satellite is important in its development and in complying with debris mitigation guidelines. Factors that must be taken into consideration include environmental perturbations, such as solar radiation pressure, the Earth's oblateness, and atmospheric drag. Other factors that affect orbital lifetime prediction are the satellite's physical properties. In this research, these perturbations and their effects on orbital lifetime, for Earth-orbiting satellites, were investigated.

In this study, orbital lifetimes were determined using the Lifetime analysis tool in Analytical Graphics' Satellite Tool Kit (STK) software, focusing on pico- and nano-satellites. The focus on these two classes of satellites is due to their perceived rapid growth and the

potential difficulty of adhering to FCC requirements for debris mitigation. The effect of solar cycle and different atmospheric density models were also explored during the analyses.

The results indicate that orbital lifetimes of pico-satellites can be significantly reduced by increasing their drag area. For instance, changing the drag area of a 1-kg satellite from 0.01 to 0.1 m^2 decreased its orbital lifetime from 22 to 3 years, an 86% reduction. At 600 km above the Earth's surface, pico-satellites with drag areas of 0.1 m^2 had minimum orbital lifetimes during years of highest solar activity. Our analysis implies that passive de-orbiting devices such as drag chutes can be effective devices on pico-satellites for addressing orbital debris mitigation. Meanwhile, the nano-satellites used in our study were between 11 to 28 kg, with drag areas from 0.08 and 0.2 m^2, which led to orbital lifetimes in centuries when launched at 750 km altitude. Values indicate that additions to the nano-satellites are needed to fulfill a 25 year orbital lifetime requirement set by the FCC.

CHAPTER 1
INTRODUCTION AND BACKGROUND

Definition of Orbital Debris

The launch of Sputnik in 1957 was the dawn of space exploration and a significant milestone in the advances in science and technology. Since that date, numerous missions and manned spacecraft have been launched and continue to be launched for scientific, educational, and technological purposes. A major effect not considered in the early years of space exploration was the contribution of artificial bodies (i.e., spent satellites and spacecraft components) to the debris population in space. Two categories of debris now exist, natural (i.e., meteoroids) and artificial (i.e., used rocket bodies). Artificial debris is also referred to as orbital debris. Orbital debris refers to man made space objects that are no longer functioning or serve any useful purpose. Prior practices and procedures have allowed unregulated growth of orbital debris, however, in recent years, the issue of orbital debris has become extremely important requiring that the space industry monitors debris orbiting the Earth and develop procedures to curtail its growth in the future.[1]

Concerns with Orbital Debris

There are several factors that have and will contribute to the growth of orbital debris, the primary contributors being (1) explosions, (2) prior practices and procedures that have involved the abandonment of spacecraft and upper stages, (3) the deposition rate of objects being sent into space, (4) collisions, and (5) future trends of small satellite usage by academia, government and industry.

First, orbital debris growth's primary cause is explosions, which produce breakups or fragments. Explosions can be accidental or intentional. Accidental explosions obtain energy from on-board energy sources. Meanwhile, intentional explosions include tests (i.e., anti-

satellite testing) or spacecraft separation. For example, in low Earth orbit (LEO), altitudes up to 2,000 km above the Earth's surface, accidental explosions of spent upper stages have been the main source of debris.[2]

Second, the next largest contributor to orbital debris has been prior practices and procedures that involved the abandonment of spacecraft and upper stages in their current orbit after the spacecraft has completed its mission or is no longer operational. The National Aeronautics and Space Administration (NASA) reported in 1995 the accumulation of approximately 1968 tons of orbital debris due to these practices.[2]

Third, assets are being launched into space at a rate that is higher than the rate at which expired assets are being removed by natural and artificial means.[3] This has led to an average growth rate in debris population of 5% per annum in LEO.[4]

Fourth, a major concern to orbital debris growth is collisions. Collisions can occur between varieties of satellite classes. Due to their large speeds, when space objects collide with each other, they may become non-operational. These masses would spatially distribute themselves producing debris fragments or debris clouds and thus add on to the total debris population. The threat of these clouds is evident by the debris created from the recently destroyed Chinese satellite, Fengyun 1-C, this past January 2007.

Last, research and trends in the past were focused on traditional large costly satellites, but are now transitioning to smaller satellites. This trend is the result of these satellites potential lower costs and advances in technology, which allows for miniaturization. The Defense Advanced Research Projects Agency (DARPA) organization is exploring fractionated spacecraft flying in formation as well as a collection of heterogeneous small satellite modules[5] performing various tasks. This trend is also seen in academia through projects such as the CubeSat and the

University Nano-satellite Program (UNP).

The CubeSat program was developed by the California Polytechnic State University in San Luis Obispo, and Stanford University's Space Systems Development lab as a mechanism to enable universities to participate in the design, launch, and operations of satellites at an affordable cost.[6] A one unit CubeSat is a 10×10×10 cm cube with a mass of 1 kg classified as a pico- satellite. Currently, these satellites typically have short operational lifetimes as compared to their orbital lifetimes and if not properly disposed after its primary mission will then contribute orbital debris.

The UNP is a joint program composing of the Air Force Research Laboratory's Space Vehicles Directorate (AFRL/VS), the Air Force Office of Scientific Research (AFOSR), and the American Institute of Aeronautics and Astronautics (AIAA). The program is a national student satellite design and fabrication competition. It also enables small satellite research and development, integration, payload development, and flight tests.[7] There are a growing number of these satellite classes planned on being sent to space and the increase can potentially contribute to the total amount in number and mass of the orbital debris population.

The growth of orbital debris has become an immediate issue as its presence in space continues to have an impact with the utilization of space assets. It is continuously monitored and modeled by agencies such as NASA and the United Nations Committee on the Peaceful Uses of Outer Space (UNCOPUOS) for study and risk assessment to future space missions. The impact, both immediate and lasting, of collisions and explosions on the orbital debris population and resultant hazards to space operations are discussed.

Explosions can produce debris fragments in large number and cause an operating spacecraft to fail, as well as produce smaller debris fragments that may degrade its performance.

Other spacecraft, hundreds of kilometers away, may also be at a great risk from these fragments due to their high velocities that may set them in very long orbit lifetimes.[2]

According to NASA, collision between large objects follows this scenario:

> First, once collisions begin to occur, it will be almost impossible to halt the process and they will occur with increasing frequency—a process referred to as collisional cascading. Second, the energies in collisional breakup are much larger than in explosive breakup, in the megajoule (a few kilograms to TNT) to gigajoule (a few metric tons of TNT) range. This energy comes from the very large amount of chemical energy used to get objects into orbit. This large amount of expended energy creates many more debris fragments in all size ranges and spreads the debris over many hundreds of kilometers of altitude. This debris may hit other satellite surfaces, carrying impact energies of hundreds of megajoules per kilogram of impactor mass. At these energies, debris less than 1 mm in diameter, typically about 1 mg of mass, can penetrate an unshielded spacecraft surface and damage sensitive surfaces such as optics or thermal radiators; debris less than 1 cm (1 gm) can penetrate even a heavily shielded surface; and debris as small as 10 cm (1 kg) can cause a spacecraft to break up into debris fragments.[2]

Consequently, the risk of collision between debris and another object has become a close concern. Abandoned spacecraft and upper stages are cases of large non-operational objects already in space for which this type of collision can occur. Computer modeling indicates that collisions between large objects in orbit will become a major source of debris within the next 3 decades, even if spacecraft launches were limited at 5 launches per year. The orbital debris that will be produced from these collisions will be small particles that are large in number and are capable of damage to operational spacecraft.[1,2]

For the purpose of this research, collision of objects in LEO is the focus. In this orbit, the standard impact velocity of medium-sized orbital debris with other objects is about 13 km/s, with an explosive potential equal to 40 times its mass of TNT. For instance, a 1-cm-diameter aluminum sphere, about 1.4 grams, has a kinetic energy equivalent to the energy released by the explosion of 0.056 kg of TNT (about 0.24 MJ). A 10-cm aluminum sphere, on the other hand, is equivalent to 56 kg of TNT (about 240 MJ). Therefore, in LEO, the energy released by small debris pieces may severely damage or destroy many spacecraft systems.[1]

Development of Mitigation Guidelines

Assessments of potential risks involved with orbital debris have led to possible solutions and abatement measures. Although removing abandoned spacecrafts, upper stages, and other orbital debris may be the most effective means in avoiding future collisions, this is not cost effective because it would require difficult maneuvering of objects in space.[2,8]

Several national and international agencies/organizations are involved in orbital debris assessment and mitigation. In 1993, the Inter-Agency Space Debris Coordination Committee (IADC) was founded "to enable space agencies to exchange information on space debris research activities, to review the progress of ongoing cooperative activities, to facilitate opportunities for cooperation in space debris research and to identify debris mitigation options"[9]. Members of the IADC consists of NASA, the Italian Space Agency (ASI), the British National Space Centre (BNSC), the Centre National d'Etudes Spatiales (CNES), the China National Space Administration (CNSA), the Deutsches Zentrum fuer Luft-und Raumfahrt e.V. (DLR), the European Space Agency (ESA), the Indian Space Research Organisation (ISRO), the Japan Aerospace Exploration Agency (JAXA), the National Space Agency of Ukrain (NSAU), and the Russian Aviation and Space Agency (Rosaviakosmos).

By February 1994, the United Nations (UN) Scientific and Technical Subcommittee agreed that international cooperation was needed to minimize the potential impact of space debris on future space missions.[9] NASA issued a comprehensive set of orbital debris mitigation guidelines in 1995.[10] The U.S. Government along with NASA, the Federal Aviation Administration (FAA), the Department of Defense (DoD), and the Federal Communications Commission (FCC) presented a set of orbital debris mitigation standard practices in a 1998 U.S. Government Orbital Debris Workshop for Industry.[11] Japan, France, Russia, and the European Space Agency (ESA) and other countries, have since followed suit with their own guidelines.[10]

President Reagan issued a directive on national space policy requiring the limitation of orbital debris accumulation on February 11 of the same year. This directive initiated the collaborative work of the U.S. and other nations to learn more about orbital debris hazards and management. An International Technical Working Group was established through this, which helped influence nations with space activities to take action in limiting orbital debris.[2]

By the year 2001, the United States Government adopted its own guideline, U. S. Government Orbital Debris Mitigation Standard Practices. [10,12] The IADC reached a consensus on a set of guidelines that were formally presented to the Scientific and Technical Subcommittee of the UNCOPUOS on February 2003.[10] In June 2004, the FCC issued its own set of mitigation rules, Orbital Debris Notice, closely following the U. S. Government Orbital Debris Mitigation Standard Practices.[13]

Several orbital debris mitigation guidelines have been in place after NASA's lead. NASA's, the U.S. Government's, the IADC's and the FCC's guidelines are summarized here with a focus on post mission disposal in LEO, for the purpose of this thesis. NASA's guideline has three general options for post mission disposal in LEO which are (1) atmospheric re-entry, (2) maneuvering to a storage orbit, and (3) direct retrieval. For option one, the guideline states to maneuver a structure into an orbit where atmospheric drag, the main nongravitational force acting on satellites in LEO,[14] will cause its lifetime to decay within 25 years after the end of its mission. The second option states to maneuver the spacecraft with final missions passing through LEO to a disposal orbit defined to be between 2500 km to 35,288 km. The last option states to perform a direct retrieval of the spacecraft from its orbit within 10 years after the end of its mission.[2]

The U.S. Government guidelines has the same three options as NASA, but with the

inclusion of human casualty risk to be limited to no greater than 1 in 10,000 upon re-entry added to option one; different disposal orbit definition for option two; and, the time period stated to be "as soon as practical" given for option three.[12] The IADC Space Debris Mitigation Guidelines has a post mission disposal section for the LEO region. The guideline gives the option for space systems to be disposed by de-orbiting, by direct re-entry, by maneuvering it to an orbit that reduces its lifetime and by direct retrieval.[15]

The FCC, which has general authority over U.S. radio communications with the exception of government radio stations, includes three methods for post mission disposal. One method is direct retrieval, which the commission currently states little relevance for this option regarding Commission-licensed space stations. Another method is to maneuver a spacecraft to a disposal or storage orbit. The storage orbit is defined to be in perigee altitudes above 2000 km and apogee altitudes below 19,700 as suggested for satellites in LEO. The FCC gives two procedures for the atmospheric re-entry option: (1) to use the spacecraft's propulsion to bring it further into the Earth's atmosphere and (2) to move the satellite to an orbit from which atmospheric drag will cause its re-entry into the Earth's atmosphere and that it will decay within 25 years after the end of its mission. For continued affordable access to space, the FCC ruled that a satellite system operator must submit an orbital debris mitigation plan before requesting space station authorization.[13]

Motivation of Research

This research, in response to the FCC ruling, investigates the different parameters that affect the orbital lifetime of pico- and nano-class satellites. These classes of satellites are increasingly gaining attention throughout the space industry due to their potential low cost and technological advances. The University of Florida has been involved with small satellite research, in particular the CubeSat, since the fall of 2004. The nano-satellites developed through

the UNP are another example of the trend in academia moving towards small satellites. The increase in number of these satellites being sent to space is a concern. The typical size, mass, and power ratios of these two classes of satellites are shown in Figure 1-1.

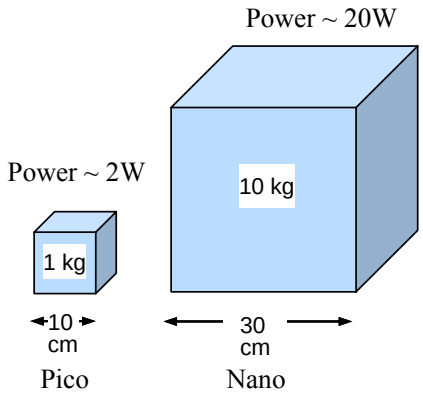

Figure 1-1. Typical pico- and nano-class satellite mass, volume and power ratios

As of May 2007, there have been 17 of the pico-class satellites referred to as CubeSats successfully launched in LEO and are namely:[16,17]

- 2003: AAU CubeSat by the Aalborg University, DTUSat by the Technical University of Denmark, CanX-1 by the University of Toronto SFL, CubeSat XI-IV by the University of Tokyo, Cute-1 by the Tokyo Institute of Technology Matunaga LSS
- 2005: NCube-2 by the University of Oslo (and others), UWE-1 by the University of Würzburg, CubeSat XI-V by the University of Tokyo
- 2006: Cute-1.7 by the Tokyo Institute of Technology Matunaga LSS, HITSat by the Hokkaido Institute of Technology
- 2007: AeroCube-2 by the Aerospace Corporation, CAPE-1 by the University of Louisiana, CP-3 and CP-4 by the California Polytechnic State University, CSTB-1 by the Boeing company, Libertad-1 by the Sergio Arboleda University, MAST by Tethers Unlimited

The CubeSat has a small mass and volume that can make a huge collision impact especially due to both the high velocity rates and concentration of spacecrafts in LEO. Figure 1-2 shows a computer generated image of the concentration of orbital debris that has been tracked in LEO (2005) courtesy of NASA. As opportunities for CubeSats to access space continue to proliferate, their contribution to the total mass may not seem substantial on a small scale. However, the

quantity of dispersed orbiting CubeSats would deter the grade of the orbit unless measures are taken to prevent this by satellite developers. Also, there are currently no enforced mitigation plans for CubeSats.

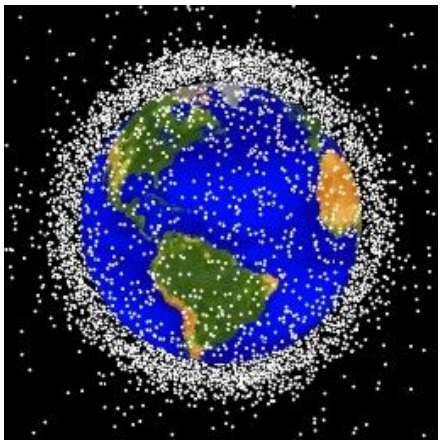

Figure 1-2. Computer generated image of orbital debris in LEO. Courtesy of NASA.[18]

The nano-satellites also have the potential to contribute to the total mass and number of orbital debris in space. The number of these types of satellite planned on being launched is increasing. Details of the properties of the nano-satellites chosen for this study are further discussed in Chapter 3. The initiative to take the necessary measures to reduce the orbital lifetime of these types of satellites, in order to prevent them from becoming orbital debris, is a step towards being responsible users of the space environment and must be taken seriously.

In Chapter 2, the equations of motion for the two-body problem and the equations that lead to orbital lifetime prediction are presented followed by some computer programs available for predicting orbital lifetime. In Chapter 3, Satellite Tool Kit (STK), the software used in this study for orbital lifetime prediction, is presented and the different parameters used for the simulation scenarios are reported. Chapter 4 elaborates on the orbital lifetime prediction results for the pico- and nano-satellites, while the conclusions and recommendations for this research are in Chapter 5.

CHAPTER 2
METHODS

In this chapter the equation of motion for the two-body problem is discussed. Brief summaries of conic sections and orbital elements are given. The equations of motion for the two-body problem with perturbations are also presented. These equations are then used to describe orbital lifetime. Some programs for orbital lifetime prediction are presented.

Two-body Problem

A model to describe a satellite's orbital motion can be developed from planetary motions. The physical motions of each planet were first described by Johannes Kepler's three laws:[19]

- First Law – The orbit of each planet is an ellipse, with the sun at a focus.
- Second Law – The line joining the planet to the sun sweeps out equal areas in equal times.
- Third Law – The square of the period of a planet is proportional to the cube of its mean distance from the sun.

The first two laws of planetary motion were published in 1609, while the third in 1619. The mathematical equations of planetary motions were not formulated until about 50 years later, through Issac Newton's second law of motion and law of universal gravitation. Newton's second law of motion states that "the rate of change of momentum is proportional to the force impressed and is in the same direction as that force"[19]. Newton's law of universal gravitation states that "any two bodies attract one another with a force proportional to the product of their masses and inversely proportional to the square of the distance between them "[19].

The equation for the second law of motion can be written as

$$\sum \vec{F} = m_i \frac{d^2 \vec{r}_i}{dt^2} \equiv m_i \frac{d\vec{v}_i}{dt} \tag{2.1}$$

The notation $\sum \vec{F}$ represents the sum of all the forces acting on a body which is equal to its

mass, m_i, times its acceleration, $\frac{d^2\vec{r}_i}{dt^2}$, measured relative to an inertial frame, and $\vec{v}_i$ is the velocity vector. Newton's law of universal gravitation can be written as

$$\vec{F}_g = G\sum_{\substack{j=1 \\ j\neq i}}^{n} \frac{m_i m_j}{r^3_{ij}}(\vec{r}_j - \vec{r}_i) \quad i = 1,...n \tag{2.2}$$

where $\vec{F}_g$ is the gravitational force on m_i due to m_j and $(\vec{r}_j - \vec{r}_i)$ is the vector from m_i to m_j. The symbol *G* represents the universal gravitational constant and has the value of 6.670×10^{-8} dyne cm^2/gm^2.[19]

The equations of motion for planets and satellites were developed from equations (2.1) and (2.2). The equations of motion are applicable for a system of two bodies, referred to as the two-body problem, where *n* = 2 in equation (2.2). An illustration of the system with bodies m_1 and m_2 is shown in Figure 2-1. Two assumptions are required to develop the equations of motion and are as follows: (1) body 1 and body 2 are spherically symmetric (this allows for the bodies to be treated as though the concentrations of their masses are at their centers) and (2) only gravitational forces are acting on the system, which act along the line joining the centers of the two bodies. An inertial reference frame is also defined to measure the motion. In Figure 2-1 the set of inertial coordinates is defined by (X, Y, Z). The position vectors of m_1 and m_2, with respect to the inertial frame, are defined as $\vec{r}_1$ and $\vec{r}_2$, respectively, so that $\vec{r} = \vec{r}_2 - \vec{r}_1$.[19]

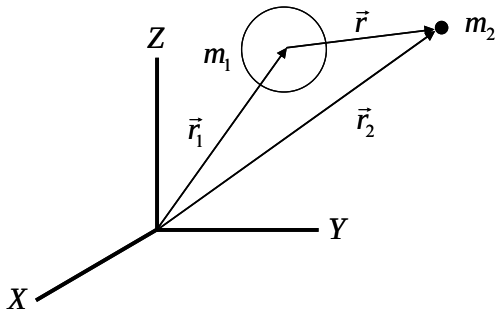

Figure 2-1. Relative motion of two-bodies

Equating Newton's second law of motion and his law of universal gravitation, for $i = 1$ and 2, after some manipulations, the governing equations of motion of m_1 and m_2 are

$$\frac{d^2\vec{r}_1}{dt^2} = G\frac{m_2}{r_{12}^3}(\vec{r}_2 - \vec{r}_1) \tag{2.3}$$

$$\frac{d^2\vec{r}_2}{dt^2} = G\frac{m_1}{r_{21}^3}(\vec{r}_1 - \vec{r}_2) \tag{2.4}$$

where $r_{12} = r_{21} = \left|\vec{r}_2 - \vec{r}_1\right| = r$, which is the distance between the two bodies. Twelve constants are required for a complete solution of these second order ordinary differential equations, but only 10 exist and thus the equations cannot be solved analytically. The two equations can be reduced to find the relative motion of body 2 with respect to body 1 by subtracting equation (2.3) from (2.4) which results in

$$\frac{d^2\vec{r}}{dt^2} = -G\left(\frac{m_1 + m_2}{r^3}\vec{r}\right) \tag{2.5}$$

where $\vec{r}$ is the position vector from m_1 to m_2. Equation (2.5) may be rewritten as

$$\frac{d^2\vec{r}}{dt^2} + \frac{\mu}{r^3}\vec{r} = \vec{0} \tag{2.6}$$

assuming that m_1 = mass of the Earth and is much greater than m_2 = mass of the satellite so that $\mu = G\left(m_1 + m_2\right) \approx Gm_1$, which is called the Earth's gravitational constant. Equation (2.6) is the equation for the relative motion of two-bodies with only gravitational forces acting upon the system describing the motion of m_2 with respect to m_1.[19] Equation (2.6) is a second order, nonlinear, vector, differential equation, that can be solved analytically, which requires six constants of integration for a complete solution from $\vec{r}_0$ and $\vec{v}_0$ or six other constants.

By conservation of angular momentum, the orbit of a satellite around the Earth can be

shown to lie on a plane. The angular momentum vector, $\vec{h}$, is then perpendicular to the orbit plane and is a constant vector. A partial solution to Equation (2.6) is easy to obtain, that tells the size and shape of the orbit. Crossing $\vec{h}$ to Equation (2.6) leads to a form of equation that can be integrated:

$$\frac{d^2\vec{r}}{dt^2} \times \vec{h} = \frac{\mu}{r^3}\left(\vec{h} \times \vec{r}\right) \tag{2.7}$$

The left side of Equation (2.7) equals $\frac{d}{dt}\left(\frac{d\vec{r}}{dt} \times \vec{h}\right)$ and the right side equals $\frac{\mu}{r}\vec{v} - \frac{\mu}{r^2}\frac{dr}{dt}\vec{r}$ and after some manipulations Equation (2.7) can be rewritten as

$$\frac{d}{dt}\left(\frac{d\vec{r}}{dt} \times \vec{h} = \mu\frac{d}{dt}\left(\frac{\vec{r}}{r}\right)\right) \tag{2.8}$$

Integrating both sides results in

$$\frac{d\vec{r}}{dt} \times \vec{h} = \mu\frac{\vec{r}}{r} + \vec{B} \tag{2.9}$$

where $\vec{B}$ is a vector constant of integration. Dot multiplying Equation (2.9) by $\vec{r}$ results in a scalar equation

$$h^2 = \mu r + rB\cos f \tag{2.10}$$

where f is the angle between $\vec{B}$ and $\vec{r}$. By solving for r, Equation (2.10) becomes

$$r = \frac{h^2/\mu}{1 + (B/\mu)\cos f} \tag{2.11}$$

and is called the trajectory equation expressed in polar coordinates.[19]

Conic Sections

Equation (2.11) is similar to the equation of a conic section, where a conic section may be defined as "a curve formed by the intersection of a plane passing through a right circular cone"[14].

The equation of a conic section can be written as

$$r = \frac{p}{1 + e\cos f} \tag{2.12}$$

and gives the magnitude of the position vector, $|\vec{r}| = r$, in terms of its location in the orbit where p is called the parameter or semi-latus rectum, e is the eccentricity, and f is the polar angle or true anomaly. The type of conic section represented by equation (2.12) is determined by the value of the eccentricity. When $e = 0$ the conic section is a circle, $0 < e < 1$ produces an ellipse, $e = 1$ generates a parabola, and $e > 1$ represents a hyperbola.

Figure 2-2 shows a geometric representation of an elliptic conic section. The figure shows the conic section having two foci, where F is the primary focus (i.e., the Earth's center) and F' is the secondary or vacant focus. C is the center of the ellipse. Half the distance between foci is the dimension c'. The dimension a is the semi-major axis and b is the semi-minor axis of the ellipse. The distance from the primary focus to the farthest point of the ellipse is called the radius of apogee, r_a, and to the closest point of the ellipse is called the radius of perigee, r_p.

From Kepler's Second Law, the time required to complete one orbit is called the orbital period, *TP*, and is expressed as

$$TP = \frac{2\pi}{\sqrt{\mu}} a^{3/2} \tag{2.13}$$

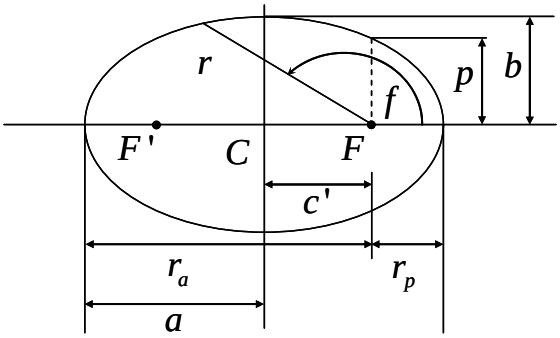

Figure 2-2. Geometry of an elliptic conic section

Orbital Elements

The six other constants of integration possible, asides from position and velocity for the solution of Equation (2.6), to describe the motion of a satellite around the Earth, are known as orbital elements or Keplerian orbital elements as shown in Figure 2-3 and are defined below (See reference 14).

- Semi-major axis (a) – Defines the size of the orbit.
- Eccentricity (e) – Defines the shape of the orbit.
- Inclination (i) – The angle between $\vec{Z}$ and angular momentum vector, $\vec{h}$.
- Right Ascension of Ascending Node (RAAN) (Ω) – "The angle from the vernal equinox to the ascending node. The ascending node is the point where the satellite passes through the equatorial plane moving from south to north. Right ascension is measured as a right-handed rotation about the pole, $\vec{Z}$."
- Argument of Perigee (ω) – "The angle from the ascending node to the eccentricity vector, $\vec{e}$, measured in the direction of the satellite's motion. The eccentricity vector points from the center of the Earth to perigee with a magnitude equal to the eccentricity of the orbit."
- Mean anomaly (M) – "The fraction of an orbit period which has elapsed since perigee, expressed as an angle. The mean anomaly equals the true anomaly for a circular orbit."

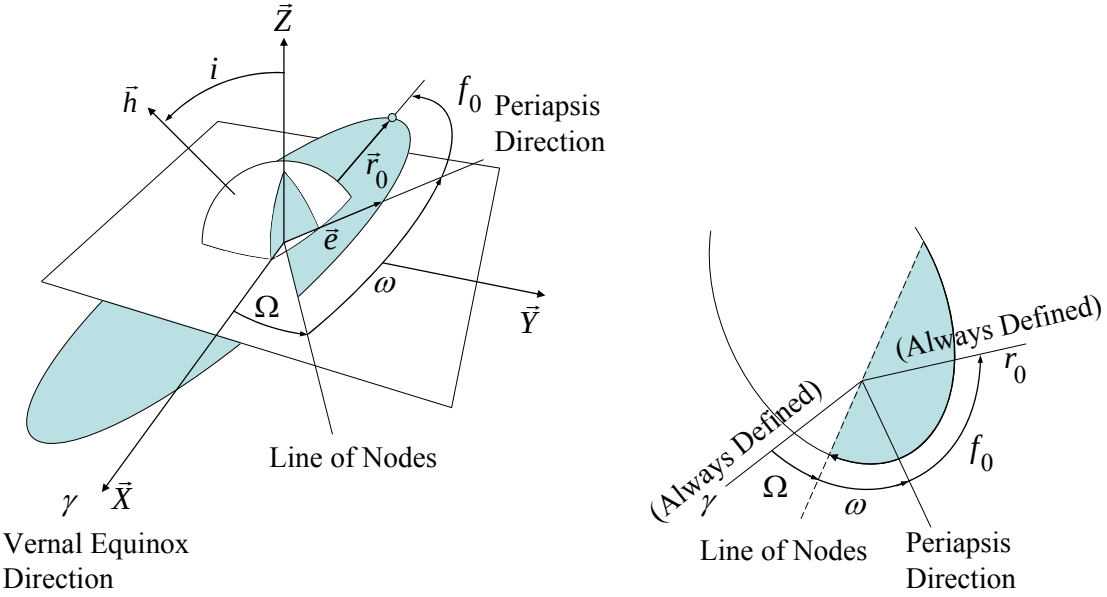

Figure 2-3. Orbital elements

Perturbations

The amount of time a satellite remains in orbit before perturbations causes its reentry into the Earth's atmosphere is the satellite's orbital lifetime and can be found from the sum of its orbital period, *TP*. The orbital period is a function of the semi-major axis. When the semi-major axis remains constant then the period is constant and the orbital lifetime is indefinite. Orbital lifetime goes towards infinity as a increases because the period gets larger. Orbital lifetime becomes finite when the semi-major axis decreases as this causes the period to decrease. The duration of a satellite's orbit with respect to the Earth is indefinite when the only forces acting on the system are gravitational forces. The orbital elements also remain constant. When other forces act on the system, however, the relative motion equation becomes

$$\frac{d^2\vec{r}}{dt^2} + \frac{\mu}{r^3}\vec{r} = \vec{a}_d \tag{2.14}$$

where $\vec{a}_d$ is the perturbing acceleration. This non-homogeneous differential equation implies that the previous "constants of motion are no longer constant. Thus, orbital lifetime can be finite when perturbations are considered. [20,21]

Some of these perturbations are atmospheric drag, solar radiation pressure, the Earth's oblateness, and other bodies (n-body effect). Factors to consider with these perturbations are solar activity, geomagnetic activity, atmospheric density, and ballistic coefficient (a function of the satellite's mass, mean cross sectional drag area, and drag coefficient). These perturbing accelerations cause a satellite's orbit to decrease and no longer be indefinite. The orbit will decay into the Earth's atmosphere and the time it takes for the decay to bring the satellite into the Earth is the satellite's orbital lifetime. In predicting the orbital lifetime of satellites, perturbations must be taken into consideration. These factors and uncertainties in the solar and

geomagnetic activities can make orbital lifetime prediction very challenging.[20,21] Some of the factors that affect lifetime are discussed here.

The Earth's upper atmosphere has a strong effect on satellites in space. The atmosphere is dynamic and is affected mostly by the sun's radiation. This solar activity heats up the atmosphere and it expands as a result. The expansion "produces a variation in density proportional to the degree of heating, which in turn depends upon solar activity"[22]. Solar activity and Sun spots vary periodically, which is commonly known as the 11-year solar cycle. The radiation from the sun is measured as a mean daily flux in the 10.7 cm (F10.7) wavelength in solar flux units (sfu).

A bulge is also created, as a result of the heating on the side of the Earth that is facing the sun. This causes "the density at a given point above the Earth to vary diurnally, as the point rotates through the bulge every 24 hours, and seasonally, as the bulge moves with the sun in latitude from winter to summer"[22]. The atmosphere is influenced by geomagnetic activity as well "through delayed heating of atmospheric particles from collisions with charged energetic particles from the sun"[23]. Satellite lifetimes are affected most by the variation in the solar cycle and the heat from radiation. Disturbances from geomagnetic activity are usually too short to affect lifetimes significantly.[14]

Atmospheric drag is the main nongravitational force that acts on a satellite in LEO.[14] Drag is part of the total aerodynamic force that acts on a body moving through a fluid such as air.[21] It acts in the direction opposite of the velocity and takes away energy from the orbit. The decrease in energy causes the orbit to decay until the satellite reenters the atmosphere. The equation for the acceleration of a spacecraft due to drag is

$$a_d = -\frac{1}{2}\rho\left(\frac{C_d A}{m}\right)v_r^2 \tag{2.15}$$

where ρ is the atmospheric density, C_d is the satellite's drag coefficient ≈ 2.2, A is the average cross-sectional area of the satellite normal to its direction of travel (drag area) , m is the mass of the satellite and v_r is the satellite's velocity relative to the atmosphere. The term $\frac{m}{C_d A}$ is the ballistic coefficient and is used as a measure of a satellite's response to drag effects.[14,23] The drag area is directly related to the satellite's shape, dimensions and attitude motion.[21] Mass is usually taken to be constant during a satellite's lifetime. When there is a mass loss, drag deceleration of the satellite increases and its lifetime is shortened.[22] The ballistic coefficient can indicate how fast a satellite will decay along with solar activity. Satellites with low ballistic coefficients tend to decay more quickly in response to the atmosphere than those with high ballistic coefficients, which progress through more solar cycles. During solar maxima satellites tend to decay more quickly and during solar minima satellites tend to decay more slowly as well. The effect of atmospheric drag is not significant to satellites with perigees below ~120 km due to the high density of the Earth's atmosphere so satellites already have such short lifetimes up to this altitude. Atmospheric drag is weak at altitudes above 600 km and thus a satellite's orbital lifetime is longer than its operational life.[14]

Solar radiation pressure influences the orbital elements by causing periodic variations to them. Satellites with low ballistic coefficients feel strong effects from this.[14] Solar radiation pressure produces acceleration in a radial direction away from the sun. The equation for solar radiation pressure may be written as

$$a_{rp} = \Gamma\left(\frac{T}{c}\right)\left(\frac{A_s}{m}\right) \tag{2.16}$$

where A_s is the satellite's average area projected normal to the direction of the sun in m^2, m is the satellite's mass in kg, T is the solar flux (SF) near the Earth, c is the speed of light, and Γ is

the satellite's reflection coefficient with a value of $0 \le \Gamma \le 4/3$. ($\Gamma = 0$ transparent; $\Gamma = 1$ perfectly absorbing; $\Gamma = 4/3$ flat, specularly reflecting.) The value of T/c can be taken as 4.5×10^5 dynes/cm^2.[24] The acceleration from solar radiation pressure is less than the acceleration from drag below 800 km altitude and greater than the acceleration from drag above 800 km, with the exception of balloon-type satellites because of large area to mass ratio.[14,21]

For the two-body equations of motion the masses were assumed to be spherically symmetric. The Earth, represented as m_1, however is not spherically symmetric, but instead has a bulge at the equator, is oblate, and is a pear shape. The Earth although can be modeled without this asymmetry by using a potential function. The acceleration of a satellite due to the central body can be found by taking the gradient of the gravitational potential function expressed as

$$\Phi = \left(\frac{\mu}{r}\right)\left[1 - \sum_{n=2}^{\infty} J_n \left(\frac{R_e}{r}\right) P_n\left(\sin L\right)\right] \tag{2.17}$$

where R_e is the Earth's equatorial radius, P_n are Legendre polynomials, L is geocentric latitude, and J_n are dimensionless geopotential coefficients also called zonal coefficients. Periodic variations occur in all orbital elements as a result of the potential generated by the Earth. The J_2 term represents the Earth's oblateness in the geopotential expansion. The J_2 perturbation has the most effect on satellites in Geosynchronous Earth Orbit (GEO), an orbit where a satellite appears to remain stationary over one location above the Earth's equator defined to be centered at an altitude of 35,788 km, and below GEO.[14] The asymmetric mass distribution of the Earth alone can not lead to orbital decay; however, it can bring about large oscillations in the orientation and shape of the orbit. These oscillations coupled with drag alters orbital lifetime.[21]

Other bodies that can affect a satellite are the sun and moon, which exert gravitational forces that also cause perturbations. Oscillations in all orbital elements and orbital plane

precession are caused by tidal forces created by the third-bodies. These forces have great effect on satellites far away from the Earth's center. These perturbations are only significant for satellites near the Earth with eccentricity greater than 0.5. The effects of the sun and moon attraction are usually neglected since most satellites near the Earth are launched into orbits with low eccentricity.[21]

Perturbation Techniques

Equation (2.14) is the general form for the relative motion of two bodies with perturbations. There are three main methods to solving the equations of motion with perturbations; special perturbation, general perturbation and semi-analytic. Special perturbation uses straightforward numerical integration of the equations of motion that includes all the essential perturbing accelerations. Two such approaches are Cowell's method and Encke's method. The numerical approach uses the position and velocity vectors of the satellite. General perturbation replaces "the original equations of motion with an analytical approximation that captures the essential character of the motion over some limited interval and which also permits analytical integration"[23]. The analytical approach usually uses the orbital elements for integration. Semi-analytic methods use a combination of the special perturbation (numerical) and general perturbation (analytic) techniques.[14,23]

Equation (2.14) is a non-homogeneous differential equation and may be solved using the method of variation of parameters. The general solution of equation (2.14) involves the homogenous solution, from equation (2.6). The homogenous solution is known and may be expressed as

$$\vec{r} = r(t,\alpha) \quad \vec{v} = \vec{v}(t,\alpha) \tag{2.18}$$

where $\vec{\alpha} = \begin{pmatrix} a & e & i & \omega & \Omega & M \end{pmatrix}$, the six constants of integration or orbital elements.

For the disturbed motion of two bodies the orbital elements are no longer constant and are governed by

$$\frac{d\vec{\alpha}}{dt} = \frac{d\vec{\alpha}}{d\vec{v}}\vec{a}_d \tag{2.19}$$

where $\vec{a}_d$ represents the perturbing accelerations. A detailed derivation on how to obtain equation (2.19) can be found in reference.[25]

After substituting the orbital elements in equation (2.19), the following variational equations, (2.20) to (2.25), are obtained:

$$\frac{da}{dt} = \frac{2e\sin f}{n\sqrt{1-e^2}}a_{dr} + \frac{2a\sqrt{1-e^2}}{nr}a_{d\theta} \tag{2.20}$$

$$\frac{de}{dt} = \frac{\sqrt{1-e^2}\sin f}{na}a_{dr} + \frac{\sqrt{1-e^2}}{na^2 e}\left[\frac{a^2\left(1-e^2\right)}{r} - r\right]a_{d\theta} \tag{2.21}$$

$$\frac{d\omega}{dt} = -\frac{\sqrt{1-e^2}\cos f}{nae}a_{dr} + \left(\frac{\sqrt{1-e^2}}{nae}\left[1+\frac{r}{p}\right]\sin f\right)a_{d\theta} - \cos i\frac{d\Omega}{dt} \tag{2.22}$$

$$\frac{d\Omega}{dt} = \frac{r\sin u}{na^2\sqrt{1-e^2}\sin i}a_{dh} \tag{2.23}$$

$$\frac{di}{dt} = \frac{r\cos u}{na^2\sqrt{1-e^2}}a_{dh} \tag{2.24}$$

$$\frac{dM}{dt} = n + \frac{1}{a^2 ne}\left[(p\cos f - 2re)a_{dr} - \left((p+r)\sin f\right)a_{d\theta}\right] \tag{2.25}$$

The symbol p is the semi-latus rectum which may also be written as $p = a\left(1-e^2\right)$, $n = \sqrt{\frac{\mu}{a^3}}$ is the mean motion, $u = f + \omega$ is the argument of latitude, a_{dr} is the component of the perturbing acceleration in the radial direction, $a_{d\theta}$ is the component in the orbital plane normal to the radial

direction, and a_{dh} is the component normal to the orbit plane, whose direction is determined from the cross product of the unit vectors $\hat{a}_{dr}$ and $\hat{a}_{d\theta}$.[25,26]

Following Belcher et. al.,[26] only long-term changes of the orbital elements are of importance in satellite lifetime analysis and so the short-term changes can be omitted or averaged out. Considering only long-term effects in this study, the satellite's instantaneous location along its orbit need not be included so that equation (2.25) can be omitted. A change of the independent variable from t to f is convenient in order to avoid some of the problems related with the solution of Kepler's equation, $M = E - e\sin E$, where E is called the eccentric anomaly. The change of variable equation is

$$\frac{df}{dt} = \frac{\sqrt{\mu p}}{r^2}\left\{1 + \frac{r^2}{\mu e}\left[a_{dr}\cos f - \left(1 + \frac{r}{p}\right)a_{d\theta}\sin f\right]\right\} \tag{2.26}$$

Due to the atmosphere, the semi-latus rectum will decrease less quickly than the semi-major axis and thus it is convenient to replace a by p so that equations (2.20) to (2.24) become

$$\frac{dp}{df} = \frac{2r^3\gamma}{\mu}a_{d\theta} \tag{2.27}$$

$$\frac{de}{df} = \frac{r^2\gamma}{\mu}\left\{a_{dr}\sin f + a_{d\theta}\frac{r}{p}\left[2\cos f + e\left(1 + \cos^2 f\right)\right]\right\} \tag{2.28}$$

$$\frac{d\omega}{df} = \frac{r^2\gamma}{\mu^e}\left\{-a_{dr}\cos f + a_{d\theta}\left(1 + \frac{r}{p}\right)\sin f\right\} - \frac{d\Omega}{df}\cos i \tag{2.29}$$

$$\frac{d\Omega}{df} = a_{dh}\frac{r^3\gamma\sin u}{\mu p\sin i} \tag{2.30}$$

$$\frac{di}{df} = a_{dh}\frac{r^3\gamma}{\mu p}\cos u \tag{2.31}$$

where

$$\gamma = \left\{ 1 + \frac{r^2}{\mu e} \left[a_{dr} \cos f - a_{d\theta} \left(1 + \frac{r}{p} \right) \sin f \right] \right\}^{-1} \tag{2.32}$$

Orbital Lifetime

The previous section discussed the relative motion of two-bodies with perturbations that must be taken into consideration for orbit lifetime prediction. The components of the perturbing accelerations must be substituted into equations (2.27) to (2.32) in order to obtain orbital lifetime calculations. Atmospheric drag, the main force affecting the satellites simulated in this study, is presented here following Belcher et. al. [26]

$$\vec{a}_d = -\frac{1}{2} \rho \left(\frac{C_d A}{m} \right) v_r \vec{v}_r \tag{2.33}$$

$\vec{v}_r$ is the satellite's velocity vector with respect to the atmosphere and may be expressed as

$$\vec{v}_r = \left(\sqrt{\frac{\mu}{p}} e \sin f \right) \hat{a}_{dr} + \left(\sqrt{\frac{\mu}{p}} (1 + e \cos f) - \omega_e r \cos i \right) \hat{a}_{d\theta} + (\omega_e r \cos u \sin i) \hat{a}_{dh} \tag{2.34}$$

where ω_e is the angular rate of rotation for the Earth and its atmosphere, $\hat{a}_{dr}$, $\hat{a}_{d\theta}$, and $\hat{a}_{dh}$ are the unit vectors in the a_{dr}, $a_{d\theta}$, a_{dh} directions, respectively. Substituting equation (2.34) into (2.33) yields

$$\begin{aligned} a_{dr_d} &= -\frac{1}{2} C_d \frac{A}{m} \rho v_r \sqrt{\frac{\mu}{p}} e \sin f \\ a_{d\theta_d} &= -\frac{1}{2} C_d \frac{A}{m} \rho v_r \left[\sqrt{\frac{\mu}{p}} (1 + e \cos f) - \omega_e r \cos i \right] \\ a_{dr_d} &= -\frac{1}{2} C_d \frac{A}{m} \rho v_r \omega_e r \cos(\omega + f) \sin i \end{aligned} \tag{2.35}$$

and

$$v_r \approx \sqrt{\frac{\mu}{p}} \sqrt{1 + e^2 + 2e \cos v} - \frac{p \omega_e \cos i}{\sqrt{1 + e^2 + 2e \cos f}} \tag{2.36}$$

The components obtained in equation (2.35) may now be substituted into equations (2.27) to (2.31). The equations are then integrated to obtain the changes in the orbital elements.

There are several programs available to perform the integration for lifetime prediction. SatLife, a stand alone software developed by Microcosm,[27] uses the satellite's initial orbit state, mass, and area as well as historical and predicted solar cycle values for its lifetime prediction. SatEvo, a program developed by Alan Pickup,[28] computes the decay of satellites from changes based on their orbital elements. NASA's Orbital Lifetime Program[24] uses the satellite's physical characteristics, launch date, and initial orbit state. Satellite Tool Kit's (STK) lifetime tool, the software used for this thesis, was developed by Analytical Graphics, Inc. (AGI) based on NASA's program.

There are three perturbations that STK takes into consideration: atmospheric drag, solar radiation pressure, and the Earth's oblateness. The drag perturbation is solved by semi-analytic techniques and the others by analytic methods. To obtain the total disturbing effects, the solutions for each differential equation obtained for each disturbing function is summed up. Initial orbit parameters need to be specified within the program in order for calculations to be performed. Integration of equations (2.27) to (2.31) is performed in order to obtain new orbital elements and is integrated over a single orbit. Once the new orbital elements are obtained then the period of the orbit can be found and used to predict lifetime. The process is repeated until a maximum orbit number is reached, specified by the user, or it reaches the Earth. The predicted lifetime result is then displayed on a pop up window by STK.[24] The next chapter discusses the lifetime program in STK in more detail.

CHAPTER 3
SIMULATIONS USING SATELLITE TOOL KIT (STK) SOFTWARE

Satellite Tool Kit (STK)

Satellite Tool Kit (STK) is a commercially available software, developed by Analytical Graphics, Inc. (AGI), and is used by national security and space professionals to perform analyses of complex mission scenarios involving land, sea, air, and space assets. STK includes integrated 2-D and 3-D graphics for visualization of aerospace objects such as satellites, launch vehicles, missiles, and aircraft. STK enables users to calculate position and orientation, evaluate inter-visibility times, and determine quality of dynamic spatial relationships among groups of objects. The software is capable of custom data product generation, including reports, graphs and Visual Data Format (VDF) files. STK can perform orbit/trajectory ephemeris generation, acquisition times, and sensor coverage analysis for any of the objects mentioned.[29]

STK Lifetime Tool

STK has a Lifetime analysis tool that estimates a satellite's orbital lifetime (i.e., the amount of time a satellite remains in orbit before atmospheric drag and other perturbations causes its reentry). The analysis tool is based on algorithms developed at NASA's Langley Research Center and the equations discussed in Chapter 2.[30] Utilization of STK's Lifetime analysis tool requires the user to input the satellite's characteristics (i.e., launch date, initial orbit, mass, cross-sectional area, and drag coefficient). The algorithm then computes drag effects by applying the satellite characteristics along with an atmospheric density model and a solar flux file (both selected by the user from a list of several options). Figure 3-1 shows the graphical user interface (GUI) for the Lifetime analysis tool.

As shown in Figure 3-1, the input for Satellite Characteristics includes Drag Coefficient, Reflection Coefficient, Drag Area, Area Exposed to Sun, and Mass. For these studies, a drag

coefficient (C_d) of 2.2 was used based on a flat plate model satellite. Typically, the Reflection Coefficient (Γ) varies between 0 and 4/3, but was maintained at 0.01 for this study (see additional discussion in the Parameter Sensitivity Study section).

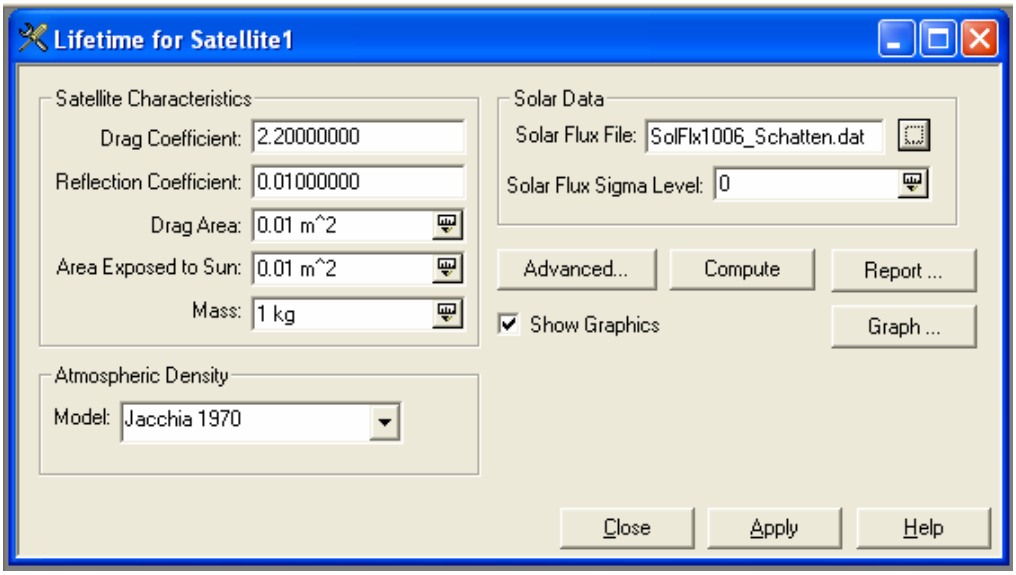

Figure 3-1. STK Lifetime tool GUI (image is courtesy of AGI).

The pico-satellite model analyzed in this study was the CubeSat with a dimension of 10×10×10 cm and a mass of 1 kg. The Drag Area of the CubeSat is 0.01 m^2, the surface area of a face of the satellite (i.e., it was assumed that one of the satellite's principal axis was aligned with its velocity vector). To investigate the effects of drag inducing devices for de-orbiting, the satellite's drag area was increased to values of 0.04 m^2, 0.06 m^2, and 0.1 m^2 (see Chapter 4).

Since there is a wide variety of nano-satellites, the following satellites from the University Nanosatellite Program (UNP) were randomly selected for the study: MR SAT and MRS SAT (University of Missouri-Rolla), FASTRAC (University of Texas at Austin), Akoya-B and Bandit-C (Washington University in St. Louis). MR SAT has a mass of 28.25 kg, hexagonal side length of 20.4 cm and height of 31.6 cm. MRS SAT has a mass of 11.45 kg, hexagonal side length of 17.6 cm and height of 19.0 cm.[31] FASTRAC consists of top and bottom hexagonal structures: the top structure of FASTRAC has a mass of 15.46392 kg, the bottom has a mass

12.5757 kg and both are 20.84 cm in height and 47.50 cm in width.[32] Akoya-B is a hexagonal structure that is 45 cm across, 45 cm tall and has a mass of about 25 kg. Bandit-C is a 12×12×18 cm cube with a mass of 2 kg [61].[33] The calculated hexagonal surface area of each satellite was used as the drag area with the exception of Bandit-C, which was calculated as its length times its width. Each satellite's mass (m), drag area (A), area exposed to Sun (A_s), and ballistic coefficient are summarized in Table 3-1.

Table 3-1. Satellite mass, drag area, and area exposed to Sun

Satellites	Mass (kg)	Drag Area* (m^2)	Area Exposed to Sun* (m^2)	Ballistic Coefficient (kg/m^2)
CubeSat	1	0.0100 (0.01)	0.0100 (0.01)	45.45
	1	0.0400 (0.04)	0.0400 (0.04)	11.36
	1	0.0600 (0.06)	0.0600 (0.06)	7.58
	1	0.1000 (0.1)	0.1000 (0.1)	4.55
MRS SAT	11.45	0.0805 (0.080478)	0.0805 (0.080478)	65.06
MR SAT	28.25	0.1080 (0.108122)	0.1080 (0.108122)	116.74
FASTRAC bottom	12.5757	0.1954 (0.195397)	0.1954 (0.195397)	28.59
FASTRAC top	15.4639	0.1954 (0.195397)	0.1954 (0.195397)	35.14
Bandit-C	2	0.0140 (0.0144)	0.0140 (0.0144)	63.13
Akoya-B	25	0.1800 (0.17537)	0.1800 (0.17537)	64.80

*Values of parameters used for analyses are in parenthesis.

Of the ten atmospheric models available in STK, only these seven were used: Jacchia 1970, Jacchia 1971, Jacchia-Roberts, CIRA 1972, MSIS 1986, MSISE 1990, and NRLMSISE 2000. Three other atmospheric models, 1976 Standard, Harris-Priester, and Jacchia 1970 Lifetime, were not used. Based on initial simulations, the 1976 Standard model is only dependent on altitude and, therefore, shows a single orbital lifetime value. Meanwhile, the Harris-Priester was found not to agree with the other models according to Woodburn and Lynch (2005).[20] The Jacchia 1970 Lifetime model was retained, in the STK version used for the analyses, for backward compatibility to previous STK versions.[34]

The simulations were performed using the solar flux file model SolFlx1006_Schatten.dat, the most recent file available during the time the simulations were performed. The numbers

associated with the flux file names represents the month and year of the data (i.e., 1006 represents October 2006 in this case). Old files are retained for regression analysis. These files contain predictions of solar radiation flux and geomagnetic index values produced by K. H. Schatten in ASCII format.[34] Updated files can be downloaded at "ftp://ftp.agi.com/pub/ DynamicEarthData" and integrated into the software. The solar flux sigma level was maintained at zero in order to use mean solar flux and weighted planetary geomagnetic index.

The accuracy and speed of the lifetime calculations are defined by selecting the Advanced button, which produces the GUI shown in Figure 3-2. The runtime of the lifetime computation can be limited by the maximum orbit duration (duration), the number of orbit revolutions (orbit count) or both. The Limit Method was set to Orbit Count in this study. The orbit count limit was adjusted to a sufficiently large value that allowed the tool to determine the lifetime of the satellite prior to termination. The number of Orbits per Calculation and the number of Gaussian Quadratures per orbit used were set at default values to provide a compromise between the amount of computation time required and the precision of the computation. The Decay Altitude is the altitude at which calculation of the satellite's orbit ceases. The default value, 65 km, and a value of 80 km were used for this research. The default options of a checked 2nd order oblateness correction and unchecked rotating atmosphere were used. The satellite's orbital elements through the duration of its lifetime can be displayed by the report and graph pane.

After calculations are performed the predicted results are displayed in a popup window that shows a date and time in Gregorian Universal Time Coordinated (UTCG), number of orbits, and lifetime in days or years down to a tenth of a decimal. It should be emphasized that the results are estimates due to atmospheric density variations and the difficulty in predicting solar activity involved with calculating a satellite's orbital lifetime.[34]

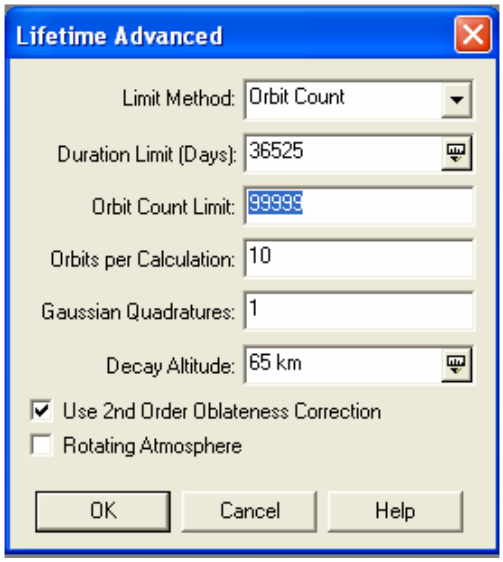

Figure 3-2. STK Lifetime Advanced option GUI (image is courtesy of AGI).

STK Satellite Properties

Figure 3-3 shows the basic orbit page GUI used to input the orbit properties for a satellite. On this page, the user chooses from a variety of analytic and numerical orbit propagators. Of the ten propagators available only two were appropriate for this analysis: J4Perturbation and High-Precision Orbit Propagator (HPOP). The J4Perturbation propagator is an analytic propagator. This propagator simply evaluates a formula in order to generate a satellite's position as a function of time in a table listing or ephemeris. The J4Perturbation considers the point mass effect of the central body, the asymmetry in the central body's gravity field, and oblateness effects. The HPOP is a numerical propagator. To generate ephemeris, HPOP uses numerical integration of the satellite's differential equations of motion. The HPOP can consider a full gravitational model, third-body gravity, solar radiation pressure, and atmospheric drag to be included for analysis. A highly precise orbit ephemeris can be generated using HPOP because of the many parameter settings available for the user. The J4Perturbation propagator was used first for testing the orbital lifetime tool and HPOP was used for more accurate orbital lifetime prediction. More detailed description of each propagator can be found in the help menu.[35]

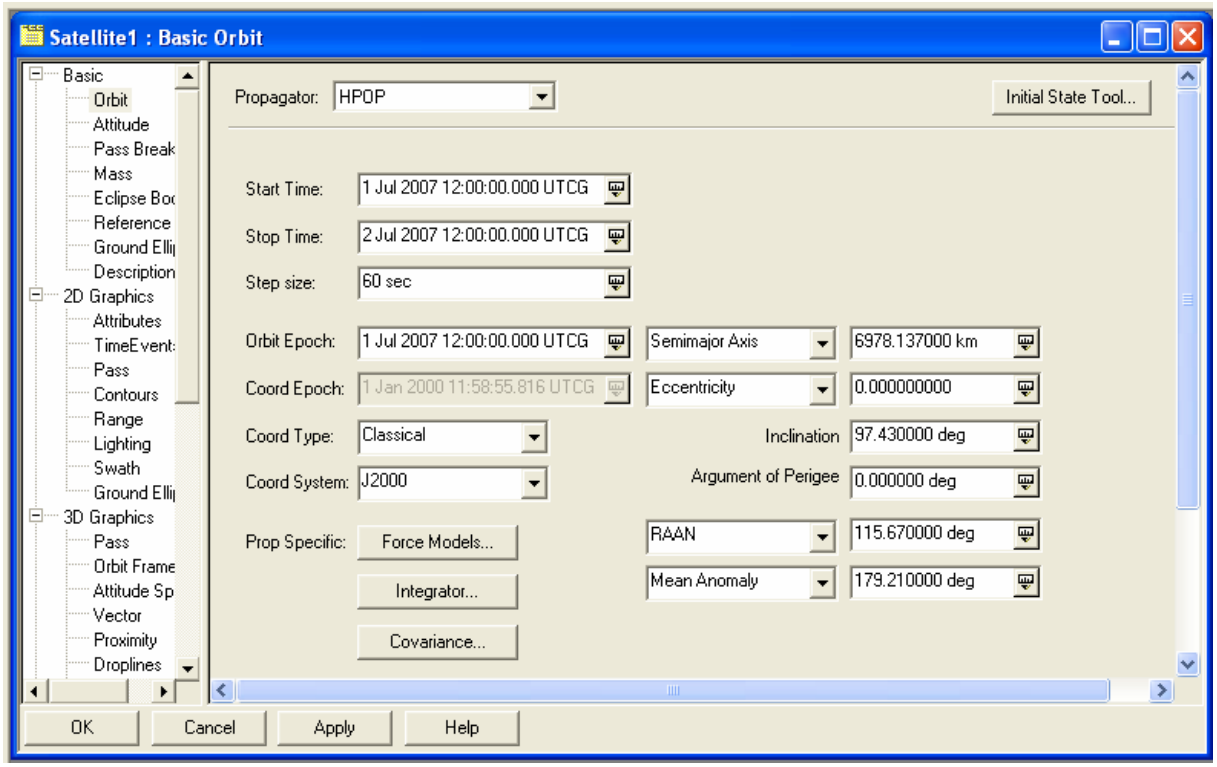

Figure 3-3. STK satellite properties GUI (image is courtesy of AGI).

A simulation Start Time, Stop Time, Step Size, and Orbit Epoch was inputted. The values for the start time, stop time, and orbit epoch are typed by the user in the format as shown in Figure 3-3. The start time corresponds with the orbit epoch and was defined to start from the default value of 1 Jul 2005 12:00:00.000 UTCG, chosen as a possible satellite launch date, and incremented by one year until 2030 to see the effect of the solar cycle on orbital lifetime. The step size was left at its default value. The stop time was defined to be a day after the start date.

The default classical (Keplerian) coordinate type and J2000 coordinate system were used for the simulations. Different sets of orbital elements and their values can be specified. Orbital elements obtained from the AeroCube-1 satellite's two line element (TLE) data from the failed launch 1 of the DNEPR vehicle were used for the pico-satellite simulations, with the exception of the eccentricity value changed to zero. The orbital elements from the mission constraint goals of the MR SAT project were used for the nano-satellite simulations.

Parameter Sensitivity Study

Simulations were performed varying different parameters such as the reflection coefficient (Γ), area exposed to Sun (A_s), drag coefficient (C_d), drag area (A), and mass (m) available within the lifetime tool to evaluate their effect on orbital lifetime prediction. A summary of the parameters that were constant for these scenarios is given in Table 3-2. The default epoch of 1 Jul 2005 12:00:00.000 UTCG was chosen as a launch date. The propagator J4Perturbation was used. The orbital elements obtained from the AeroCube-1 two line element (TLE) were used. The Jacchia-Roberts atmospheric density model and a decay altitude of 80 km were used.

Table 3-2. Orbital lifetime sensitivity simulation parameters

Parameters	Figure 3-4 to 3-8
Altitude (km):	550
Epoch Start Date:	1 Jul 2005 12:00:00.000 UTCG
Propagator:	J4Perturbation
Semimajor Axis (km):	6927.248793
Eccentricity:	0.0064
Inclination (deg):	97.43
Argument of Perigee (deg):	189.63
RAAN (deg):	115.67
Mean Anomaly (deg):	349.58
Atmospheric Density Models:	Jacchia-Roberts

Two parameters were found not to have significant effect on orbital lifetime, namely the reflection coefficient (Figure 3-4) and area exposed to Sun (Figure 3-5). As discussed in Chapter 2, these are directly proportional to the acceleration from solar radiation pressure, which was stated as being less effective than drag below altitudes of 800 km. In this thesis, analyses were performed at altitudes of 750 km and lower, where such parameters are expected not to affect orbital lifetime. Consequently, the reflection coefficient was maintained at 0.01, while the area exposed to Sun value was kept the same as the satellite's drag area. number of orbits, and lifetime in days or years with one significant digit after the decimal of the value

Four curves are shown in Figure 3-4 representing drag coefficients of 2.0 (blue-diamond),

2.05 (pink-square), 2.1 (green-triangle), and 2.2 (aqua-cross). For each curve, the reflection coefficient was varied to values of 0, 0.3, 1.0, and 1.8 while the other parameters were kept at a constant value as seen in the legend. Three curves are shown in Figure 3-5 representing drag coefficients of 2.0 (blue-diamond), 2.1 (pink-square), and 2.2 (green-triangle). The area exposed to Sun was varied from 0.05, 0.5, and 1 m^2 for each curve. The other parameters were kept at a constant value as seen in the legend. Both graphs show slopes close to zero, indicating that orbital lifetime is not affected by the reflection coefficient and the area exposed to Sun.

The results from varying the drag coefficient, drag area, and mass are shown in Figures 3-6 to 3-8. Figure 3-6 shows a graph of the orbital lifetime vs. drag coefficient. In this graph, the drag coefficient was increased to values of 1.8 to 2.5 while the other parameters were kept at constant values as seen in the legend. Figure 3-7 shows a graph of orbital lifetime vs. drag area. In this graph, the drag area was increased to values of 0.05 to1 m^2. Three curves were obtained using drag coefficients values of 2.0 (blue-diamond), 2.1 (pink-square), and 2.2 (green-triangle), while holding the other parameters constant as seen in the legend. All three curves show a decrease in orbital lifetime. Figure 3-6 shows the dependence of orbital lifetime on the drag coefficient. Figure 3-7 shows a dependence of orbital lifetime on drag area.

Figure 3-8 shows orbital lifetime vs. mass. In this graph, the value of the mass was increased to values of 1 to 5 kg while the other parameters were kept at constant values as seen in the legend. The graph shows an increase in orbital lifetime as a result of the simulation. This graph shows the dependence of orbital lifetime on mass. The three figures (Figure 3-6 to 3-8) show the dependence of the orbital lifetime on the three parameters with the given scenario. The three parameters C_d, A, and m make up the ballistic coefficient, which is expected to affect orbital lifetime as defined in Chapter 2. For the studies performed in Chapter 4, 0.01 m^2 as area

exposed to Sun and 0.01 as reflection coefficient value were used because the sensitivity studies show them to be invariant.

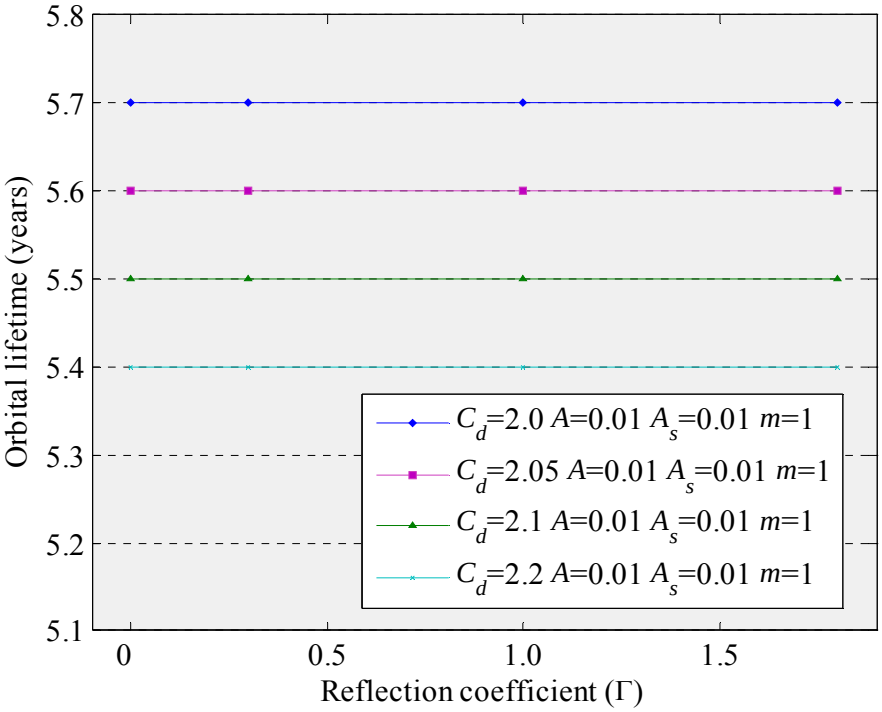

Figure 3-4. Orbital lifetime vs. reflection coefficient

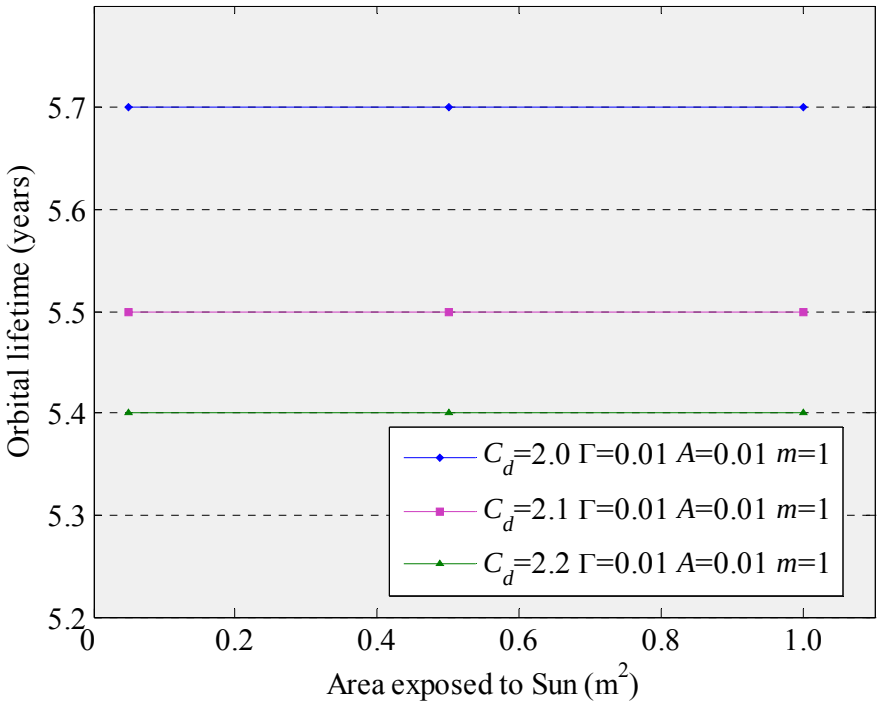

Figure 3-5. Orbital lifetime vs. area exposed to Sun

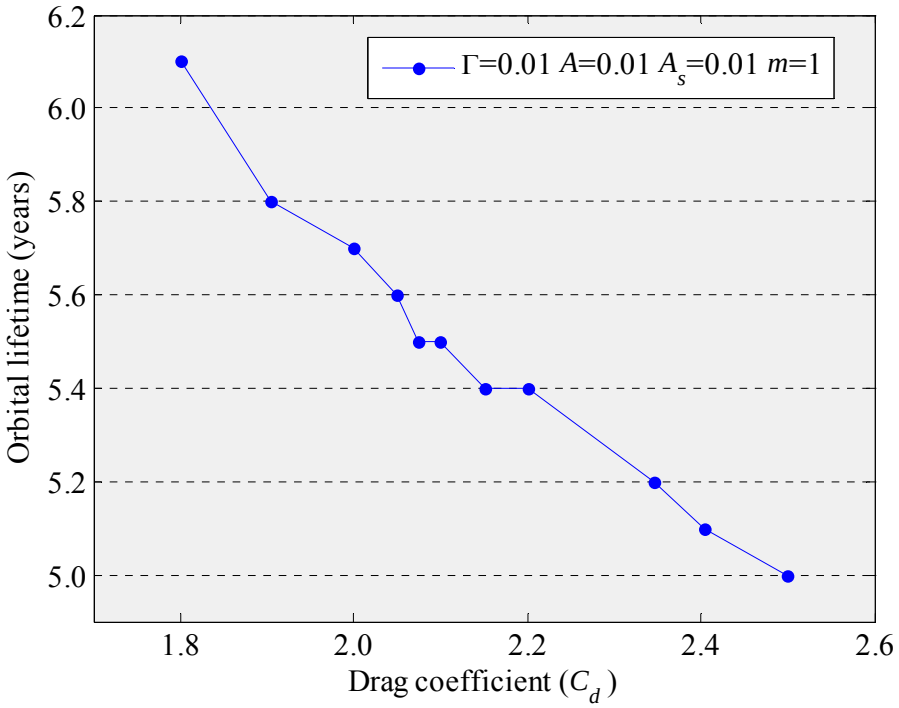

Figure 3-6. Orbital lifetime vs. drag coefficient

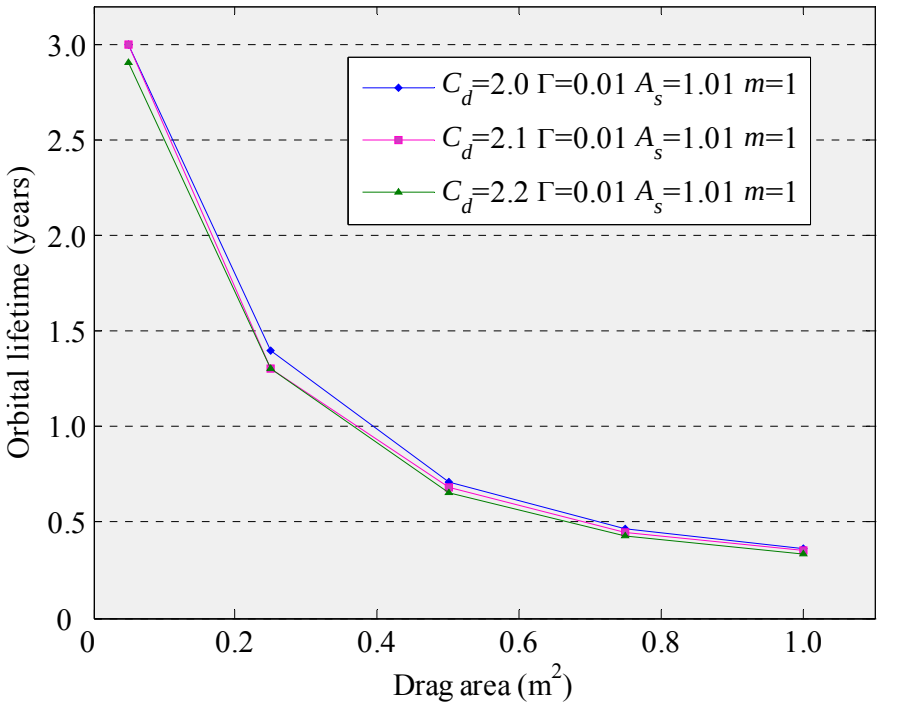

Figure 3-7. Orbital lifetime vs. drag area

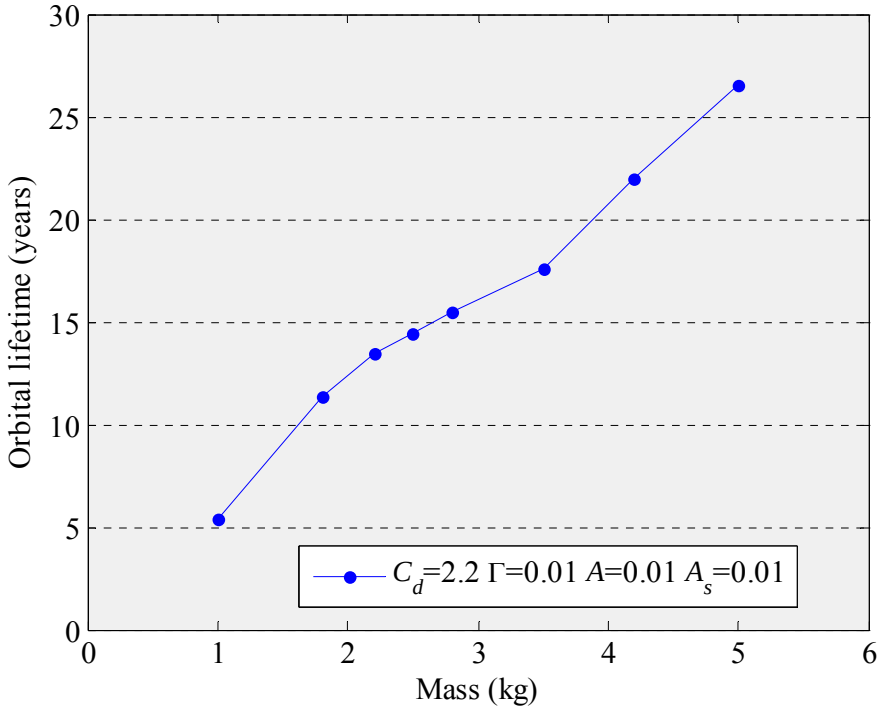

Figure 3-8. Orbital lifetime vs. mass

CHAPTER 4
RESULTS AND DISCUSSION

Simulations of orbital lifetimes for pico- and nano-satellites were performed. The results, which are presented here, were used to study the effects of different parameters have on their lifetimes. The CubeSat volume and mass are constant parameters; in order to reduce its lifetime, the impact of increasing its cross-sectional area was investigated. The volume and mass of the nano-satellites in this study varied; thus, the impact of different launch altitudes on each nano-satellites' lifetime was studied. For both analyses, different launch years were considered to see the effect of the 11-year solar cycle. Different atmospheric density models were also explored to determine maximum, minimum, and average orbital lifetime values per launch year.

Pico-satellite Results

Four scenarios were simulated for the CubeSat, with varying drag areas of 0.01, 0.04, 0.06, and 0.1 m^2, which will be referred to as satellite A, B, C, and D, respectively. The CubeSat simulation parameters are summarized in Table 4-1. An epoch start date of "1 Jul 2007 12:00:00.000 UTCG" was chosen as initial launch date and incremented yearly until 2030 to determine the effect of the solar cycle, with peaks, known as solar maxima, occurring around 2012 and 2023, and valleys, known as solar minima, at 2007, 2018, and 2029. From 2007 to 2030, a solar cycle is determined from one minimum to the next. These solar maxima and minima correspond to the years of highest and lowest solar radiation flux values, respectively, within the solar flux file "SolarFlx1006_Schatten.dat". The orbital elements for these simulations closely follow the AeroCube-1 elements, with the exception of changing the eccentricity to zero. A 600-km initial altitude was used since this value falls within the range at which the CubeSats would have been released from the DNEPR launch vehicle. Meanwhile, a decay altitude of 80 km was used for the pico-satellite analyses.

Table 4-1. CubeSat simulation parameters

Parameters	Satellites A and C	Satellites B and D
Altitude (km):	600	600
Epoch Date:	1 Jul 2007 12:00:00.000 UTCG to 1 Jul 2030 12:00:00.000 UTCG	1 Jul 2007 12:00:00.000 UTCG to 1 Jul 2030 12:00:00.000 UTCG
Propagator:	HPOP	HPOP
Semimajor Axis (km):	6978.137	6978.137
Eccentricity:	0	0
Inclination (deg):	97.43	97.43
Argument of Perigee (deg):	189.63	189.63
RAAN (deg):	115.67	115.67
Mean Anomaly (deg):	349.58	349.58
Drag Coefficient:	2.2	2.2
Reflection Coefficient:	0.01	0.01
Drag Area (m^2):	0.01 and 0.06 see figures	0.04 and 0.1 see figures
Area Exposed to the Sun (m^2):	Same as drag area respectively	Same as drag area respectively
Mass (kg):	1	1
Atmospheric Density Models:	Jacchia 1970, Jacchia 1971, Jacchia-Roberts, CIRA 1972, NRLMSISE 2000, MSISE 1990, MSIS 1986	Jacchia 1970, Jacchia 1971, Jacchia-Roberts

Seven atmospheric density models were used for satellite A (Figure 4-1) and satellite C (Figure 4-2). The data show trends for certain atmospheric density models, producing maximum, minimum and average orbital lifetime values per launch year. For the pico-satellites, orbital lifetimes for four consequent years, starting at 2007, were analyzed for satellites B and D, using the seven atmospheric density models. From these results, those models that produced maximum, minimum and close to average orbital lifetime values were determined; these were then used for the rest of the simulations in order to reduce the analysis time.

The results for satellites A, B, C, and D (Figure 4-3) were plotted using the average lifetime values as a curve, while maximum and minimum orbital lifetime values are shown as error bars. The orbital lifetime for satellite A ranged from 17 to 27 years, with an average curve value of 22 years, while that for satellite B is between 2.5 and 9 years, with a mean of 6 years. The lifetime for satellite C varied from 1 to 8 years, with an average of 4 years, while that for satellite D were 1 to 5.6 years, with a mean of 3 years. As expected, the orbital lifetimes for satellites B,

C, and D were shorter compared to satellite A due to their low ballistic coefficients.[14]

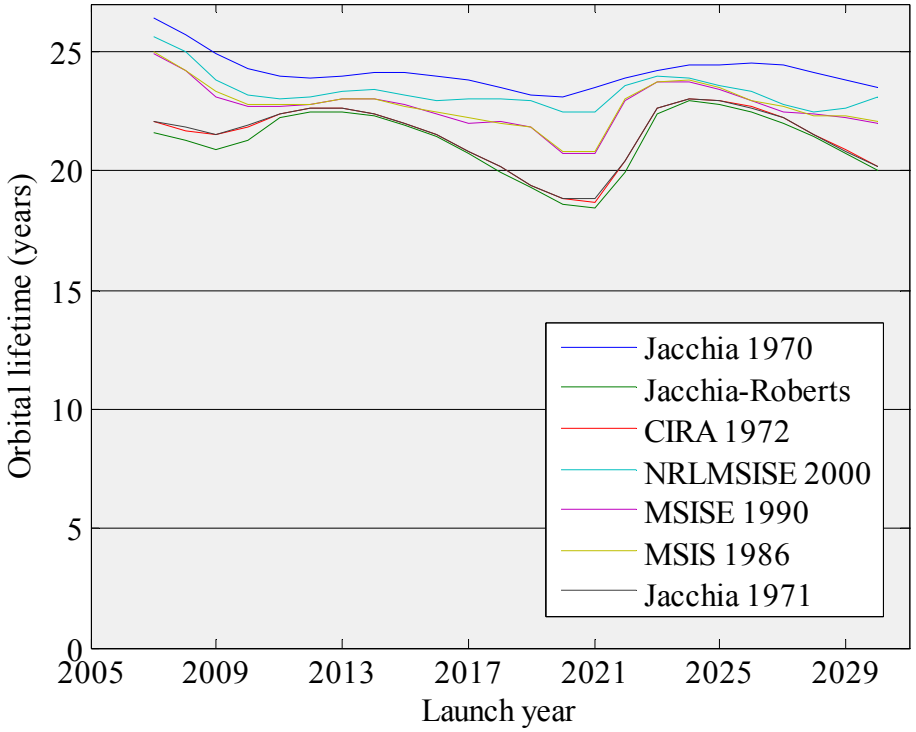

Figure 4-1. Orbital lifetime results for satellite A using seven atmospheric density models

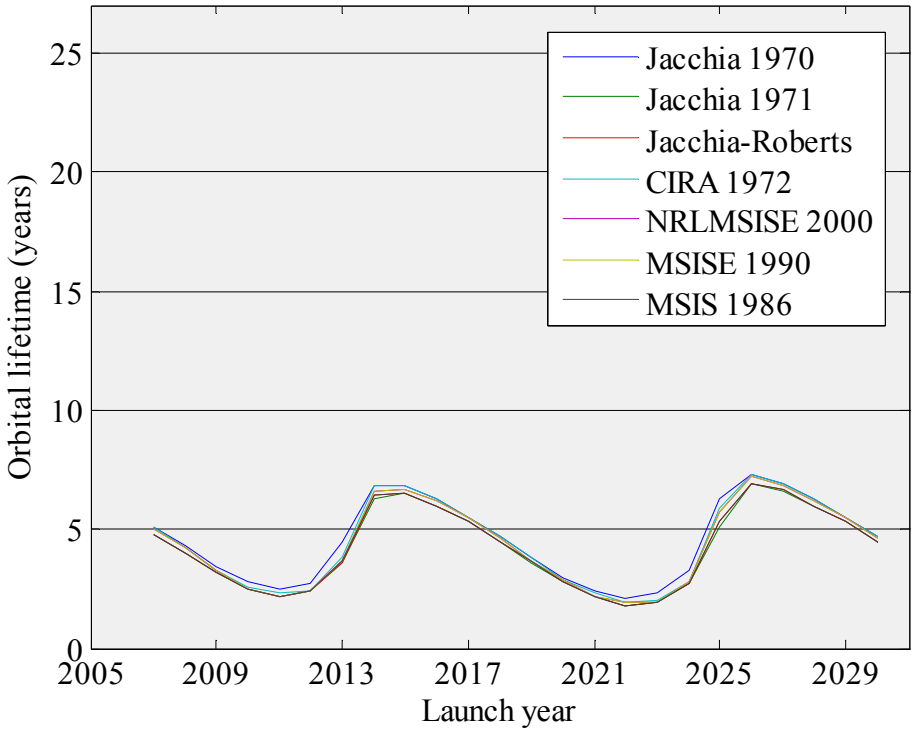

Figure 4-2. Orbital lifetime results for satellite C using seven atmospheric density models

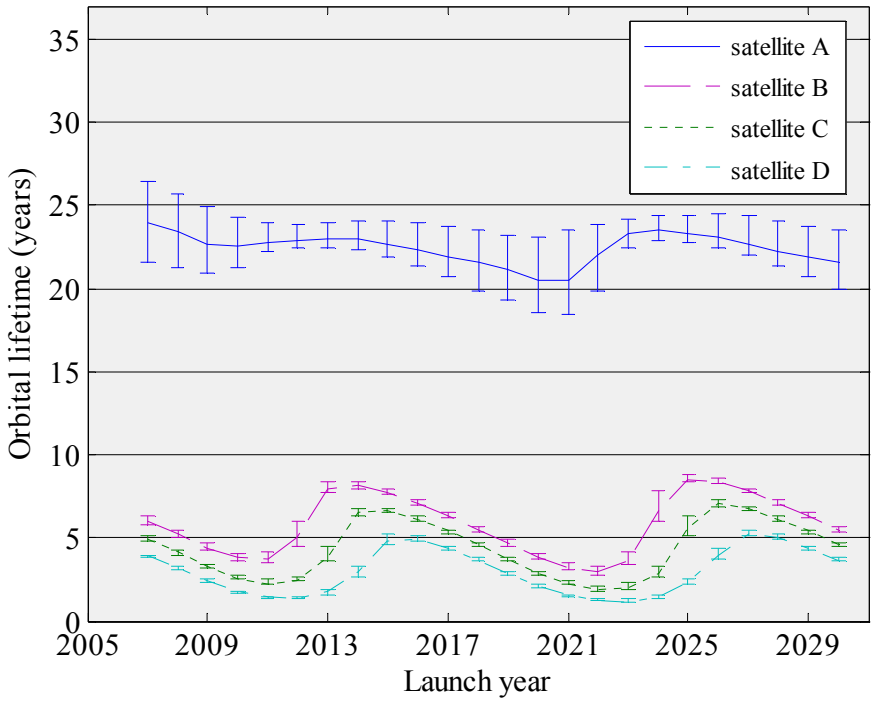

Figure 4-3. Orbital lifetime results for satellites A, B, C, and D at 600-km initial altitude

A 75% reduction in orbital lifetime can be seen as the drag area is enlarged from 0.01 to 0.06 m^2, when comparing the values for satellites A and C. A reduction of at least 40% can be seen by comparing the average orbital lifetime of satellite B to D, 30% from satellite B to C and about 25% from satellite C to D. The orbital lifetime for the CubeSat is greatly minimized when the drag area is increased to ten times its original size.

Orbital lifetime minima occur at about 2010 and 2021 for satellite A, at 2011 and 2022 for satellites B and C, and at 2012 and 2023 for satellite D (corresponding to solar cycle maxima). Analyses show orbital lifetimes of 23, 5.0, 2.4, and 1.4 years for satellite A, B, C and D, respectively, for a launch at 2012. Varying orbital lifetimes results from differences in the satellites' ballistic coefficients, the highest of which is observed for Satellite A (see Table 3-1), followed by B, then C, and minimum for D. Due to the high ballistic coefficient of satellite A, its orbit does not decay as rapidly[14] as the others; moreover, it pushes through at least 2 solar cycle minima at 2018 and 2029 and a maximum at 2023. Satellite B encounters a solar cycle

maximum at 2012 and reenters the atmosphere a year before the next cycle minimum. Satellite C and D experience a solar maximum only at 2012 and their orbits decays within the following 3 years. The orbits of satellites B, C, and D decay rapidly when launched during a solar maximum due to their low ballistic coefficients.[14]

Nano-satellites Results

The nano-satellite simulation parameters are summarized in Table 4-2 for MR SAT and MRS SAT, Table 4-3 for FASTRAC, and Table 4-4 for Akoya-B and Bandit-C. The epoch start of "1 Jul 2007 12:00:00.000 UTCG" was chosen as a possible launch date and incremented by a year until 2030 to see the effect of the solar cycle. For all the simulations, a default decay altitude of 65 km was used. Each satellite's orbital lifetime was simulated at two different altitudes and inclination: (1) at 350-km altitude and 51.6º inclination, similar to the orbit of a typical international space shuttle mission; and, (2) 750-km altitude and 57º inclination, obtained from the mission constraint goals of the MR SAT project. Atmospheric density models for the simulations were selected by means of the same methods used for satellite B and D. The results were plotted using the average lifetime values as the curve, and the maximum and minimum values as error bars.

Simulations were also performed to obtain orbital lifetimes for MR SAT, studying the effect of different initial altitudes. The parameters used are summarized in Table 4-5. An epoch start date of "1 Jul 2007 12:00:00.000 UTCG" was chosen as a possible launch date and incremented by yearly until 2030 to see the effect of the solar cycle. The simulation begins at 350-km initial altitude and is incremented by 50 km until 750 km. An inclination of 51.6º was used. A decay altitude of 65 km was used. Atmospheric density models used for the simulations were determined by the same method as for satellite B and D per launch altitude. For each launch year, the maximum and minimum orbital lifetime values are represented as error bars and the

average lifetime values as a curve obtained from the atmospheric density model results. These values were then used to plot the orbital lifetime versus altitude for MR SAT.

Table 4-2. MR SAT and MRS SAT simulation parameters

Parameters	Figure 4-4	Figure 4-5
Altitude (km):	350	750
Epoch Date:	1 Jul 2007 12:00:00.000 UTCG to 1 Jul 2030 12:00:00.000 UTCG	1 Jul 2007 12:00:00.000 UTCG to 1 Jul 2030 12:00:00.000 UTCG
Propagator:	HPOP	HPOP
Semimajor Axis (km):	6728.137	7128.137
Eccentricity:	0	0
Inclination (deg):	51.6	57
Argument of Perigee (deg):	0	0
RAAN (deg):	0	0
Mean Anomaly (deg):	0	0
Drag Coefficient:	2.2	2.2
Reflection Coefficient:	0.01	0.01
Drag Area (m^2):	MR SAT = 0.108122 MRS SAT = 0.080478	MR SAT = 0.108122 MRS SAT = 0.080478
Area Exposed to the Sun (m^2):	MR SAT = 0.108122 MRS SAT = 0.080478	MR SAT = 0.108122 MRS SAT = 0.080478
Mass (kg):	MR SAT = 28.25 MRS SAT = 11.45	MR SAT = 28.25 MRS SAT = 11.45
Atmospheric Density Models:	Jacchia-Roberts, CIRA 1972, NRLMSISE 2000	Jacchia 1970, Jacchia-Roberts, MSIS 1986

Table 4-3. FASTRAC simulation parameters

Parameters	Figure 4-6	Figure 4-7
Altitude (km):	350	750
Epoch Date:	1 Jul 2007 12:00:00.000 UTCG to 1 Jul 2030 12:00:00.000 UTCG	1 Jul 2007 12:00:00.000 UTCG to 1 Jul 2030 12:00:00.000 UTCG
Propagator:	HPOP	HPOP
Semimajor Axis (km):	6728.137	7128.137
Eccentricity:	0	0
Inclination (deg):	51.6	57
Argument of Perigee (deg):	0	0
RAAN (deg):	0	0
Mean Anomaly (deg):	0	0
Drag Coefficient:	2.2	2.2
Reflection Coefficient:	0.01	0.01
Drag Area (m^2):	top = 0.195397 bottom = 0.193597	top = 0.195397 bottom = 0.193597
Area Exposed to the Sun (m^2):	top = 0.195397 bottom = 0.193597	top = 0.195397 bottom = 0.193597
Mass (kg):	top = 15.4639 bottom = 12.5757	top = 15.4639 bottom = 12.5757
Atmospheric Density Models:	Jacchia-Roberts, CIRA 1972, NRLMSISE 2000	Jacchia 1970, Jacchia-Roberts, NRLMSISE 2000, MSIS 1986

Table 4-4. Akoya-B and Bandit-C simulation parameters

Parameters	Figure 4-8	Figure 4-9
Altitude (km):	350	750
Epoch Date:	1 Jul 2007 12:00:00.000 UTCG to 1 Jul 2030 12:00:00.000 UTCG	1 Jul 2007 12:00:00.000 UTCG to 1 Jul 2030 12:00:00.000 UTCG
Propagator:	HPOP	HPOP
Semimajor Axis (km):	6728.137	7128.137
Eccentricity:	0	0
Inclination (deg):	51.6	57
Argument of Perigee (deg):	0	0
RAAN (deg):	0	0
Mean Anomaly (deg):	0	0
Drag Coefficient:	2.2	2.2
Reflection Coefficient:	0.01	0.01
Drag Area (m^2):	Akoya-B = 0.17537 Bandit-C = 0.0144	Akoya-B = 0.17537 Bandit-C = 0.0144
Area Exposed to the Sun (m^2):	Akoya-B = 0.17537 Bandit-C = 0.0144	Akoya-B = 0.17537 Bandit-C = 0.0144
Mass (kg):	Akoya-B = 25 Bandit-C = 2	Akoya-B = 25 Bandit-C = 2
Atmospheric Density Models:	Jacchia-Roberts, CIRA 1972, NRLMSISE 2000	Jacchia 1970, Jacchia-Roberts, MSIS 1986

Table 4-5. MR SAT with different initial altitudes simulation parameters

Parameters	Figure 4-10
Altitude (km):	350 to 750
Epoch Date:	1 Jul 2007 12:00:00.000 UTCG to 1 Jul 2030 12:00:00.000 UTCG
Propagator:	HPOP
Semimajor Axis (km):	6728.137 to 7128.137
Eccentricity:	0
Inclination (deg):	51.6
Argument of Perigee (deg):	0
RAAN (deg):	0
Mean Anomaly (deg):	0
Drag Coefficient:	2.2
Reflection Coefficient:	0.01
Drag Area (m^2):	0.108122
Area Exposed to the Sun (m^2):	0.108122
Mass (kg):	28.25
Atmospheric Density Models:	Jacchia 1970, Jacchia 1971, Jacchia-Roberts, CIRA 1972, NRLMSISE 2000, MSISE 1990, MSIS 1986

The results for MR SAT and MRS SAT (Figure 4-4), with an initial altitude of 350 km, show orbital lifetime values between 140 and 370 days for the former, with an average curve value of 247 days, and between 80 and 210 days for the latter, with an average curve of

141 days. Orbital lifetime minima for the average curves in Figure 4-4 occur at 2012 and 2023 for both satellites. On the other hand, the results at 750-km initial altitude (Figure 4-5) show orbital lifetime values between 460 and 540 years for MR SAT, with an average curve value of 495 years, and between 250 and 300 years for MRS SAT, with an average curve value of 269 years. The lifetime minima for the average curve in Figure 4-5 occur at 2011 and 2021 for MR SAT, and at 2011 and 2020 for MRS SAT.

At an initial altitude of 350 km, the results for the FASTRAC top and the bottom satellites (Figure 4-6), show orbital lifetime values for FASTRAC top is between 50 and 125 days, with an average curve value of 86 days, and from 40 to 110 days for the bottom, with an average curve value of 72 days. Orbital lifetime minima for the average curves in Figure 4-6 occur at 2012 and 2023 for both satellites. On the other hand, results at 750-km initial altitude (Figure 4-7) show orbital lifetime values between 140 and 165 years, with an average curve value of 151 years for the top satellite, and from 110 to 135 years for the bottom satellite, with an average curve value of 122 years. Orbital lifetime minima for the average curves in Figure 4-7 occur at about 2011 and 2021 for the top satellite and at about 2010 and 2020 for the bottom satellite.

The results for Akoya-B and Bandit-C at an initial altitude of 350 km (Figure 4-8) show orbital lifetime values between 86 and 210 days with an average curve value of 141 days for both satellites. Orbital lifetime minima for the average curves in Figure 4-8 occur at 2012 and 2023 for both satellites. Meanwhile, the results at 750-km initial altitude (Figure 4-9) show orbital lifetime values between 255 and 295 years for Akoya-B, with average curve value 270 years, and from 250 to 285 years for Bandit-C, with an average curve value of 263 years. Orbital lifetime minima for the average curves in Figure 4-9 occur at 2011 and 2022 for Akoya-B, and at about 2010 and 2021 for Bandit-C.

The orbital lifetimes of the nano-satellites are in centuries at 750-km initial altitude, in contrast to less than 400 days at 350-km initial altitude. For both initial altitudes, the FASTRAC bottom satellite, having the lowest ballistic coefficient of the nano-satellites studied, had shortest orbital lifetime values; meanwhile MR SAT has the longest as a result of having the highest ballistic coefficient.

The orbital lifetimes for MR SAT at varying initial orbit is shown in Figure 4-10. Its average lifetime at 500 km is 11 years, more than twice the lifetime at 450 km, and more than 5 times compared to that at 400 km. This pattern continues up to 750-km initial orbit. At about 550 km, the curves merge as they progress through several solar cycles, making the launch date insignificant.at higher altitudes.[14] The pattern indicates orbital lifetimes greater than 25 years at altitudes greater than 550-km.

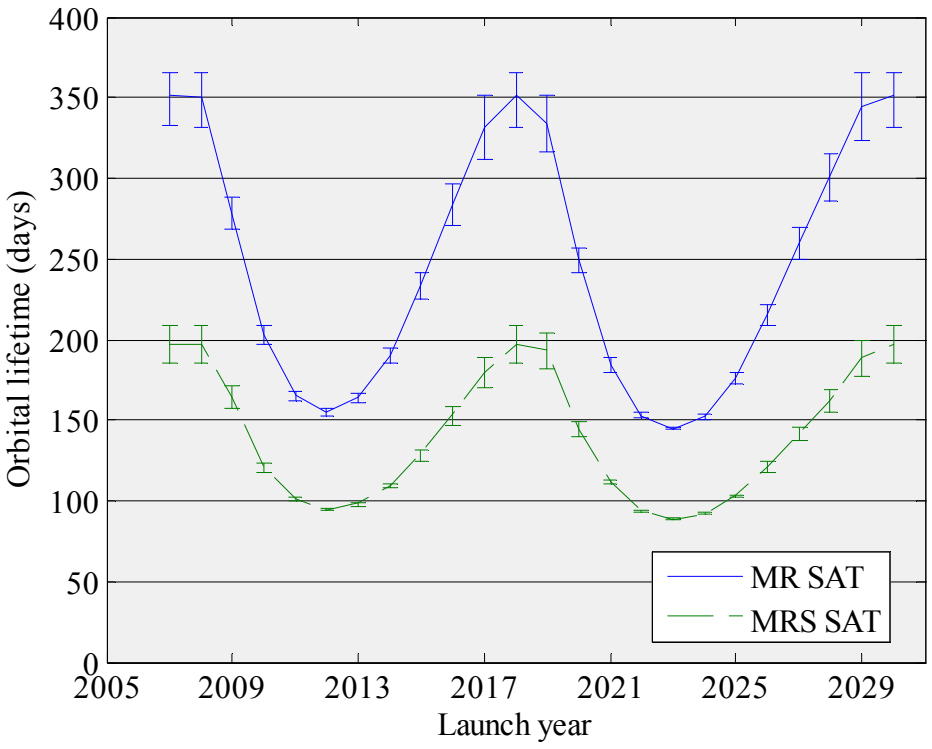

Figure 4-4. Orbital lifetime for MR SAT and MRS SAT at 350-km initial altitude

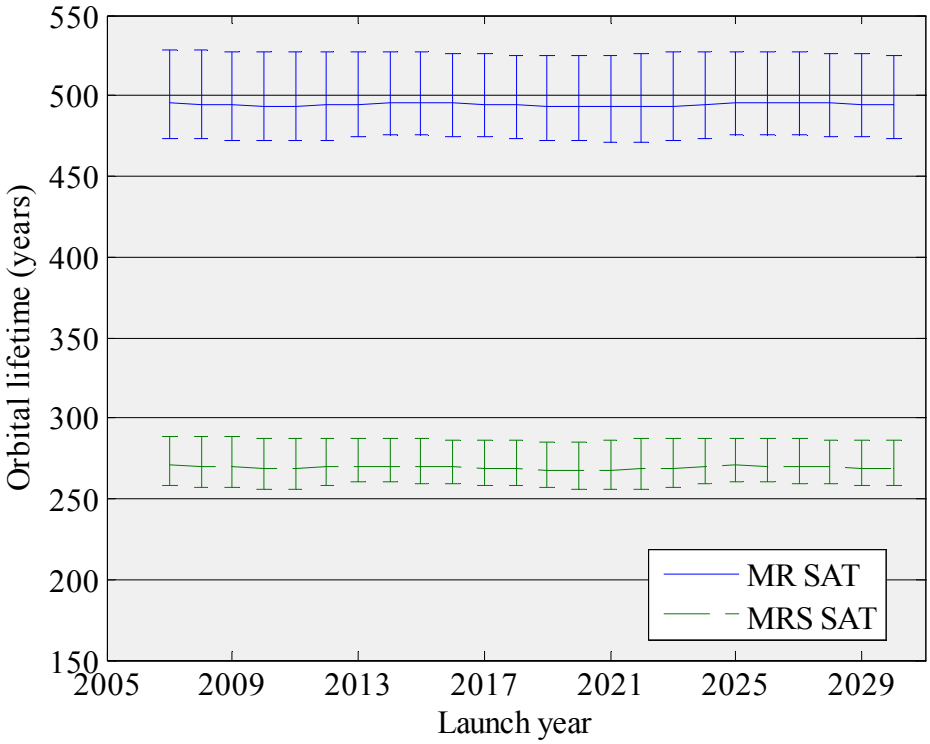

Figure 4-5. Orbital lifetime for MR SAT and MRS SAT at 750-km initial altitude

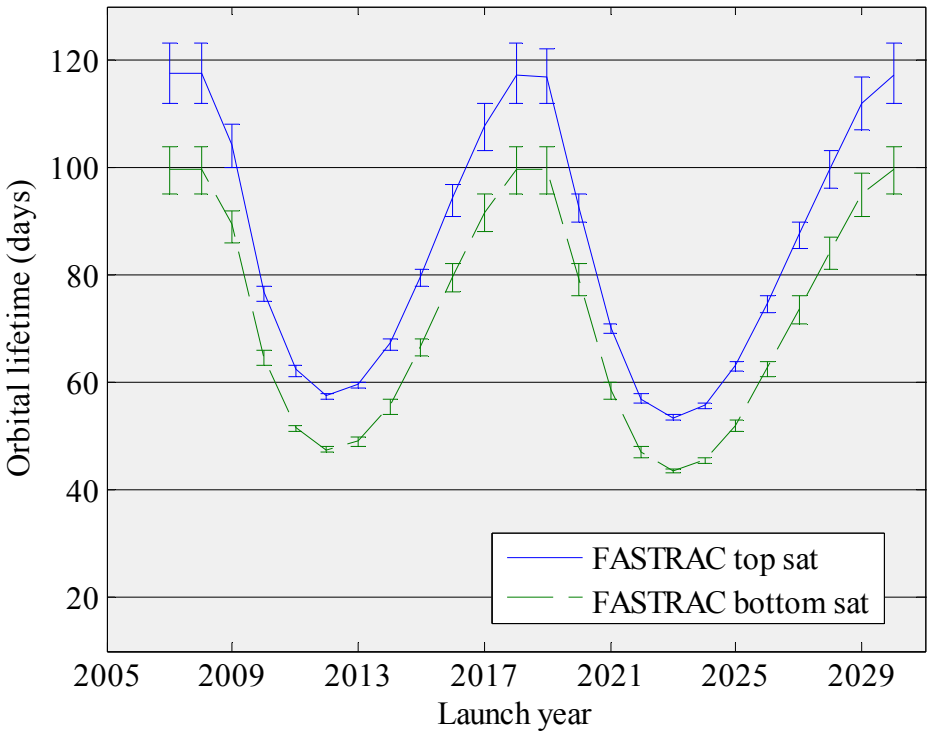

Figure 4-6. Orbital lifetime for the FASTRAC satellites at 350-km initial altitude

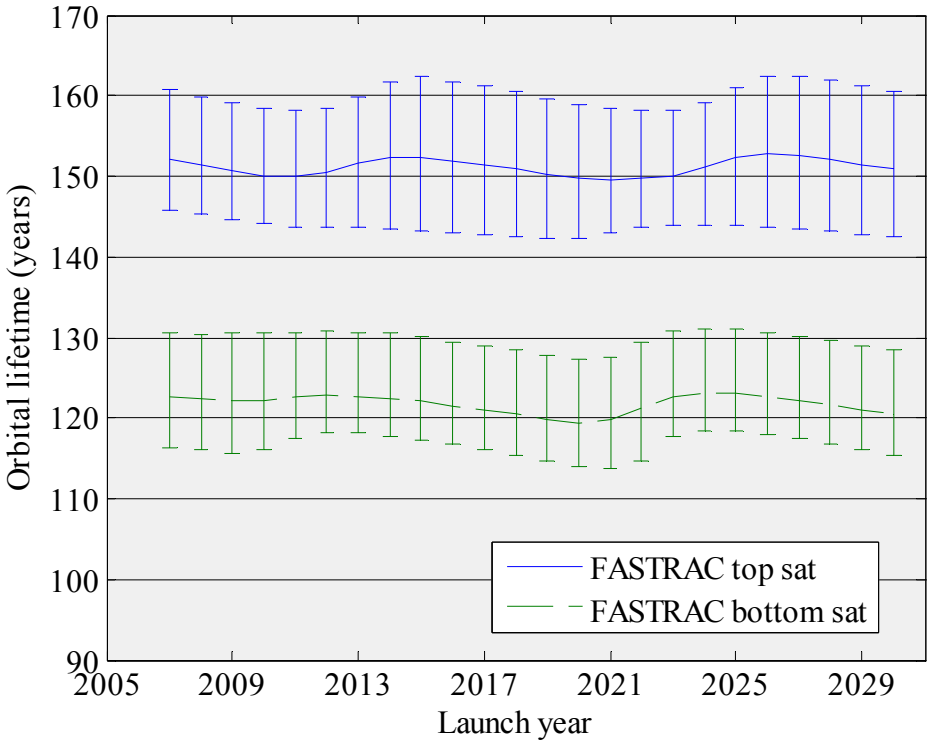

Figure 4-7. Orbital lifetime for the FASTRAC satellites at 750-km initial altitude

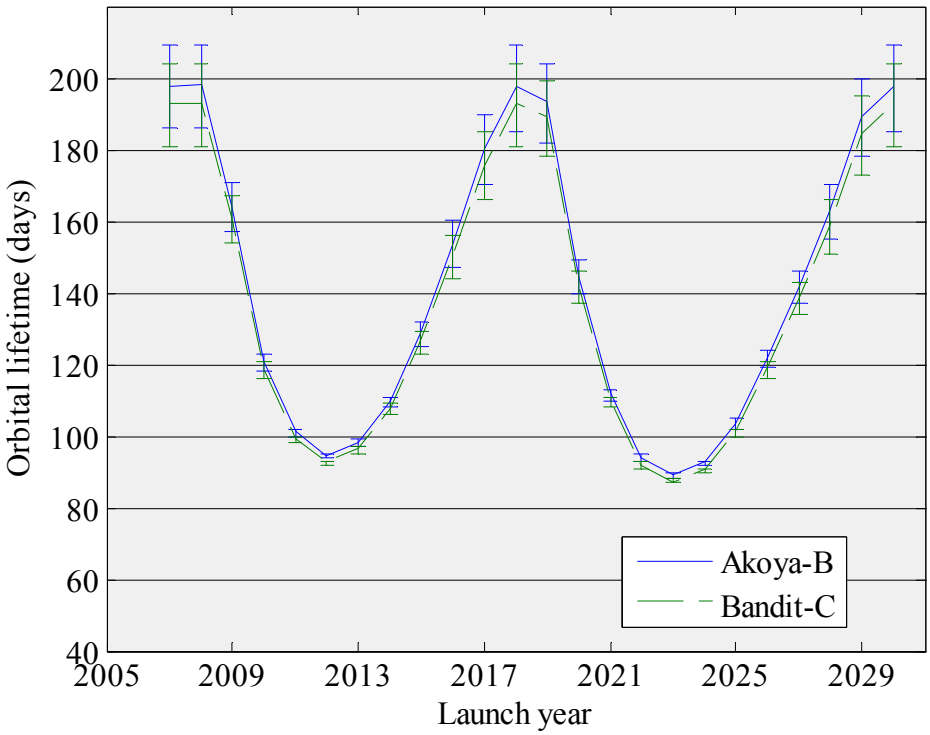

Figure 4-8. Orbital lifetime for the Akoya-B and Bandit-C at 350-km initial altitude

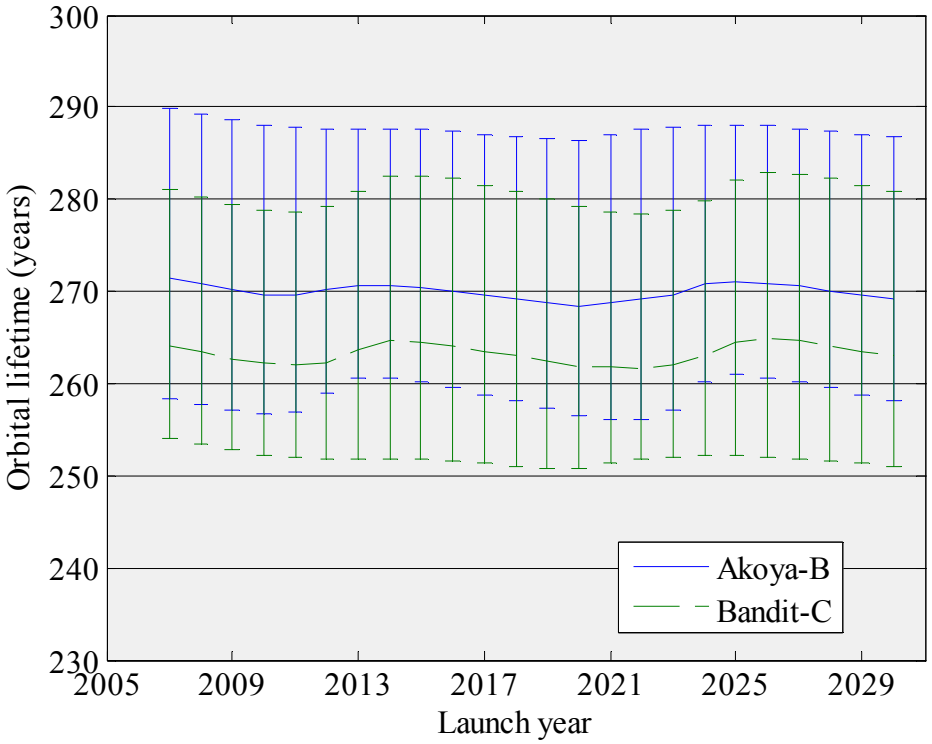

Figure 4-9. Orbital lifetime for the Akoya-B and Bandit-C at 750-km initial altitude

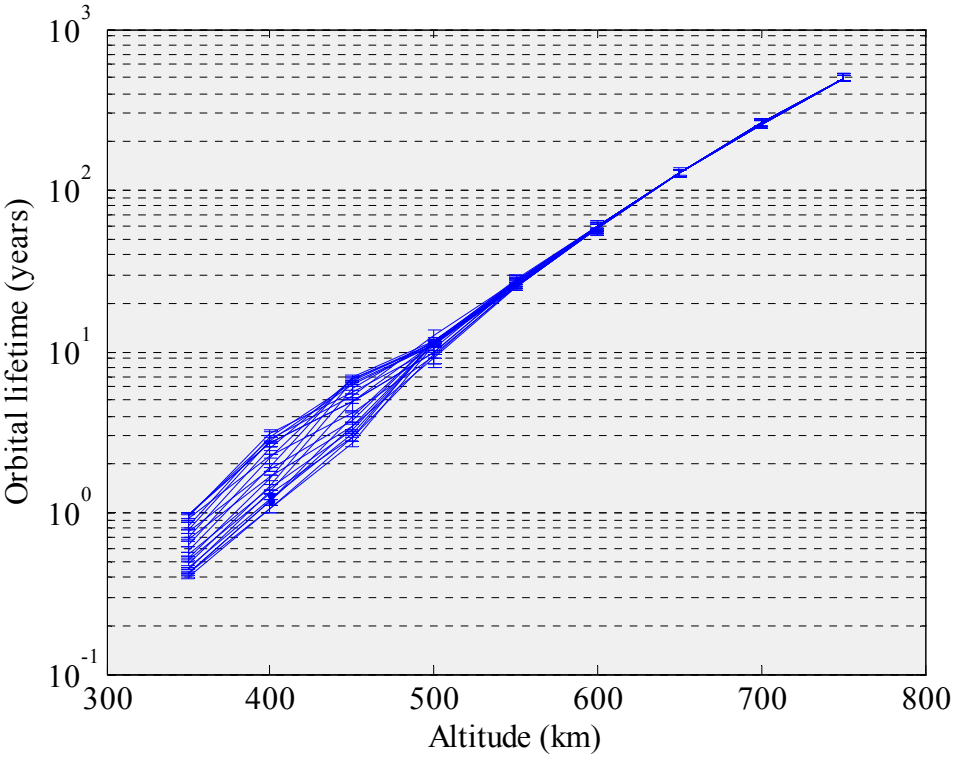

Figure 4-10. Orbital lifetime for the MR SAT using different initial altitudes

CHAPTER 5
CONCLUSION AND RECOMMENDATIONS

Conclusions

Lifetime analyses of pico- and nano-satellites were conducted using the Satellite Tool Kit (STK) orbital Lifetime tool. The pico-satellite analyses were performed on the standard CubeSat developed by CalPoly and Stanford, whereas the nano-satellite analyses were performed on three randomly selected satellites from the University Nano-satellite Program (UNP). Typical mission scenarios for these two classes of satellites were investigated. Since the prediction of orbital lifetime is not an exact science, parameters which have an effect on the prediction were varied to provide ranges of expected lifetimes for the different scenarios.

The results indicate that orbital lifetimes of pico-satellites can be significantly reduced by increasing their drag area from 0.01, to 0.04, 0.06 or 0.1 m^2. The longest that the CubeSat is predicted to stay up in orbit at a 600 km altitude with a drag area of 0.01 m^2 is approximately 27 years, which is slightly above the FCC debris mitigation guidelines. The longest that the CubeSat is predicted to stay in orbit at a 600 km altitude with a drag area of 0.04 m^2 is about 8.8 years, 0.06 m^2 is about 7 years, and 0.1 m^2 about 5.5 years. Changing the drag area of a 1-kg satellite from 0.01 to 0.1 m^2 decreased its orbital lifetime from an average of 22 to 3 years and results in 86% reduction. The results show that changing the drag areas to 0.04 or 0.1 m^2 did not make a significant difference to the reduced total amount of lifetime of the satellite than the drag area of 0.06 m^2. At 600 km above the Earth's surface, a pico-satellite with drag area of 0.1 m^2 had minimum orbital lifetimes during years of highest solar activity due to its low ballistic coefficient. At this same altitude, pico-satellites with smaller drag areas, which results in higher ballistic coefficient, responded more slowly to the solar activity and as a result the orbital lifetime minimums appear shifted from solar maximum years. This analysis implies that passive

de-orbiting devices such as drag chutes can be effective devices for addressing orbital debris mitigation. The analyses also imply that in order to obtain minimum orbital lifetimes to set the launch year of the satellite corresponding with high solar activity that is at solar maximum.

The nano-satellites used in this study were between 11 to 28 kg, with drag areas from 0.08 and 0.2 m^2. The results of the nano-satellites analyses, with a launch altitude of 350 km, show that the orbital lifetimes are in number of days. At this altitude the satellites will reenter the atmosphere in a short amount of time. These lifetime values will meet the FCC mitigation guidelines. The results of the nano-satellites analyses, with an altitude of 750 km, show that the orbital lifetimes are in centuries. At this high altitude the nano-satellites' orbital lifetime will not meet the FCC mitigation guidelines. Values indicate that additions to the nano-satellites are needed to fulfill the 25 year orbital lifetime requirements at this altitude. The nano-satellites in high orbit, above 500 km, have a problem of potentially becoming a debris space. The nano-satellites do not have a volume or mass requirement as the CubeSats, therefore these were kept constant respectively per satellite and only the effect of a change in altitude on their orbital lifetimes were investigated.

Recommendations

There are different parameters to consider with prediction of long-term orbital lifetime and its reduction. Satellites properties (i.e., geometry, mass and the solar activity, have significant effects on these. For mission operations the implementation of an aerobraking technique for both CubeSats and nano-satellites, that is a change in their drag area, should be further investigated. For mission planning the consideration of proposed satellites to be launched during the solar maximum time period should be further investigated.

LIST OF REFERENCES

1.National Research Council (U.S) Committee on Space Debris, "Orbital Debris: A Technical Assessment," National Academy Press, Washington, DC, 1995, Chaps. 4, 8.

2."NASA Safety Standard: Guidelines and Assessment Procedures for Limiting Orbital Debris," NSS 1740.14, August 1995.

3.Flury, W., "Space Debris," *Preparing for the Future* [online], Vol. 4, No. 4, 1994, http://esapub.esrin.esa.it/pff/pffv4n4/ppfflunr4.htm [retrieved 26 June 2007].

4.Aerospace Corporation, Center for Orbital and Reentry Debris Studies, "Space Debris Basics: What is the Future Trend?," http://www.aero.org/capabilities/cords/debris-future.html [accessed 26 June 2007].

5.Walker, S. H., ""Responsive" Access and Infrastructure," *Proceedings of DarpaTech 2005*, Defense Advance Research Project Agency (DARPA), Anaheim, CA, August 2005, pp. 203-207.

6.Calpoly, CubeSat, "Mission Statement", http://cubesat.atl.calpoly.edu/pages/home/mission-statement.php [accessed on 30 June 2007].

7.AFOSR, AFRL Space Vehicles, AIAA, NASA, SMC Det 12, "About the University Nanosatellite Program," http://www.vs.afrl.af.mil/UNP/About.html [accessed on 19 July 2007].

8.Orbital Debris Program Office, NASA Johnson Space Center, "Orbital Debris Education Package," http://www.orbitaldebris.jsc.nasa.gov/library/EducationPackage.pdf [retrieved 11 July 2007].

9."Technical Report On Space Debris," United Nations, (A/AC.105/720), New York, 1999.

10. Orbital Debris Program Office, NASA Johnson Space Center, "Orbital Debris Mitigation," http://www.orbitaldebris.jsc.nasa.gov/mitigate/mitigation.html [accessed 27 June 2007].

11. "U.S. Government Begins Orbital Debris Meetings with Industry," *The Orbital Debris Quarterly News*, Vol. 4, No. 4, 1999, p. 4.

12. "U. S. Government Orbital Debris Mitigation Standard Practices" at the Johnson Space Center [online], 1997, http://www.orbitaldebris.jsc.nasa.gov/library/USG_OD_Standard_Practices.pdf [accessed 1 July 2007].

13. "In the Matter of Mitigation of Orbital Debris," Federal Communications Commission, FCC 04-130, Washington, DC, June 2004, p. 2.

14. Wertz, J. R., and Larson, W. J., *Space Mission Analysis and Design*, 3rd ed., Microcosm Press, Torrence, CA, 1999, Chaps. 5, 6, 8.

15. “IADC Space Debris Mitigation Guidelines,” Inter-Agency Space Debris Coordination Committee, IADC-02-01, October 2002.

16. Calpoly, CubeSat, “Dnepr Launch Vehicle Status - Integrated for Launch”, http://cubesat.atl.calpoly.edu/pages/missions/dnepr-launch-2/satellite-status.php [accessed 30 June 2007].

17. AMSAT, “Cubesat Information,” http://www.amsat.org/amsat-new/satellites/cubesats.php [accessed 27 June 2007].

18. Orbital Debris Program Office, NASA Johnson Space Center, “Orbital Debris Graphics,” http://www.orbitaldebris.jsc.nasa.gov/photogallery/beehives.html#leo [accessed 27 June 2007].

19. Bate, R. R., Mueller, D. D., and White, J. R., “Two-body Orbital Mechanics,” *Fundamentals of Astrodynamics*, Dover Publications, Inc., New York, 1971, Chap. 1.

20. Woodburn, J., and Lynch, S., “A Numerical Study of Orbital Lifetime (revised),” *Proceedings of the 2005 AAS/AIAA Astrodynamics Specialists Conference*, Paper No. AAS 05-297, Lake Tahoe, CA, August 2005.

21. De Lafontaine, J., and Garg, S. C., “A review of satellite lifetime and orbit decay prediction,” *Proc. Indian Acad. Sci. (Engg. Sci.)*, Vol. 5, Pt. 3, September 1982, pp. 197-258.

22. Ladner, J. E., and Ragsdale, G. C., “Earth Orbital Satellite Lifetime,” NASA TN D-1995, January 1964.

23. Vallado, D. A., “Special Perturbation Techniques,” *Fundamentals of Astrodynamics and Applications*, 2nd ed., Microcosm Press, El Segundo, CA, 2001, Chap. 8.

24. Orr, L.H., “User’s Guide for Langley Research Center Orbital Lifetime Program,” NASA TM-87587, September 1985.

25. Battin, R. H., “Variation of Parameters,” *An Introduction to the Mathematics and Methods of Astrodynamics, Revised Edition*, Revised ed., American Institute of Aeronautics and Astronautics, Inc., Reston, VA, 1999, Chap. 10.

26. Belcher, S. J., Rowell, L. N., and Smith, M. C., “Satellite Lifetime Program,” The Rand Corporation, RM-4007-NASA, April 1964.

27. Space Mission Analysis and Design, “SatLife Stand-Alone Module v1.0,” http://www.smad.com/software/agimo3.html [accessed 21 May 2007].

28. Alan Pickup, “Satellite tracking and decay information,” http://www.wingar.demon.co.uk/satevo [accessed 21 June 2007].

29. Analytical Graphics, Inc., “About AGI,” http://www.agi.com/corporate [accessed 27 June 2007].

30. Analytical Graphics, Inc., "STK Editions," http://www.agi.com/products/desktopApp/stkFamily/editions/index.cfm?tab=key [accessed 27 June 2007].

31. University of Missouri-Rolla, "Conceptual Design of the *MR SAT* Tethered Satellite Project at the University of Missouri-Rolla: 1.0 Structures," http://web.umr.edu/~mrsat/docs.html [accessed 12 February 2007].

32. Holt, G., Stewart, S., Mauldin, J., Campbell, T., Eckhoff, P., Yeldell, S., Greenbaum, J., Linford, M., Diaz-Aguado, M., Wang, T., Berthold, T., Lightsey, E. G., Raja, L. L., Ebinuma, T., "FASTRAC Mission Plan: Formation Autonomy Spacecraft with Thrust, Rel-Nav, Attitude and Crosslink," The University of Texas at Austin, Austin, TX, December 2005.

33. Washington University, "Welcome to the Washington University Nanosat Page," http://www.me.wustl.edu/faculty/mas/nanosat [accessed 12 February 2007].

34. Analytical Graphics, Inc., "Lifetime Tool," http://www.agi.com/resources/help/stk613/helpSystem/stk/tools-11.htm [accessed 1 July 2007].

35. Analytical Graphics, Inc., "Satellite Orbits," http://www.agi.com/resources/help/stk613/helpSystem/stk/vehSat_orbitTab.htm [accessed 1 July 2007].

BIOGRAPHICAL SKETCH

The author was born in Quezon City, Philippines. She immigrated to the United States in Illinois on October 15, 1988. She received her bachelor's degree in Electrical Engineering on December 2002 from the University of Illinois at Chicago. In August 2007, she moved to Florida to attend the University of Florida in Gainesville. She received her master's degree in Mechanical Engineering in December 2007 with a concentration in dynamics and control.